CHARACTERIZATION OF RF PROPAGATION IN METAL PIPES FOR PASSIVE RFID SYSTEMS

by

DARMINDRA DANARAJ ARUMUGAM

Presented to the Faculty of the Graduate School of

The University of Texas at Arlington in Partial Fulfillment

of the Requirements

for the Degree of

MASTER OF SCIENCE IN ELECTRICAL ENGINEERING

THE UNIVERSITY OF TEXAS AT ARLINGTON

December 2007

ACKNOWLEDGEMENTS

When I first started working in the newly branded Texas RF Innovation and Technology Center, I knew very little about the probable road I have now taken, the people I was going to be best of friends with and most importantly the knowledge I was going to grasp in this extremely short venture called the masters degree. At that point about a year and a half ago, I was indifferent to the fact that I was going to work with Daniel Engels. However, Dan's ideas on the world often pervaded the room when we were in discussions, and were extremely infectious. Eventually I realized that Dan's need to invade the world with knowledge and alas intelligence, had also become my dream. As my advisor, Dan allowed the flexibility and push as well as motivation and constant source of excitement. For all those reasons and for exposing me to an entirely new and exciting field, I wish to thank Daniel Engels. Dan has always taken excessive amounts of time through his terribly busy schedules to help me learn the curves. Through this nurturing process, I have learned more than I could have ever dreamed of and have acquired focus for many other goals in my life. For all this and for all that he is as an advisor and friend, I wish to thank Dan again.

I must also thank Stephen Gibbs for allowing the room for my growth within UTA, which without would have made it very hard for me to pursue my need to learn and work to my fullest. Steve engaged me often in both intellectual thoughts on the world and on life. I am also very thankful to Steve for introducing me in the summer of

2006 to Dan, which marked the beginning of my thesis and research life. For the influence and help throughout the last 3 years of my life, I wish to thank Steve.

I would also like to thank the other very important individuals in my life through this process. John Priest and Richard Billo allowed me in many ways to grow into the individual that I am today. They allowed for the nurturing advices and room for growth, as well as the push when Dan was away. For all this and for teaching the ways of dealing with the world, I wish to thank John and Rick. I would also like to thank Marlin Mickle for accepting my constant bombardment of his mailbox and more importantly for thoroughly reading my thesis. Marlin's comments on my papers always made me think broadly and allowed me to understand the gaps in my thought process and writing. For this and for supporting my interest, I wish to thank Marlin.

Finally, I would like to thank my family and friends for making my life at UTA a truly enjoyable experience. I would like to thank my sister Deva, her husband Kumar and my two little nephew and niece, Devan and Denice for putting up with me through this process. I would also like to thank my brother Devin, and sisters, Molka, Lally and Levinnya for constantly inquiring about my research and supporting me through this process. Last but not least, I would like to thank my father and mother for painstakingly helping me through my entire education process and for always making sure I had a plan and goal in life. Thanks so much!

October 25, 2007

ABSTRACT

CHARACTERIZATION OF RF PROPAGATION IN METAL PIPES

FOR PASSIVE RFID SYSTEMS

Publication No. _____

Darmindra Danaraj Arumugam, M.S.

The University of Texas at Arlington, 2007

Supervising Professor: Dr. Daniel W. Engels

In this paper we collect and extend the theory of radio frequency (RF) propagation as it relates to propagation within metal cylinders, or circular pipes. This work is motivated by a need to understand the operation of UHF radio frequency identification (RFID) systems when the tags are placed within the pipes. These circular pipes are shown to be similar to metal tube waveguides which are either hollow or filled with air. We derive the Bessel function that is used to identify the propagation constants, the different transverse electric and transverse magnetic modes, cut-off frequencies and the multi-mode attenuation. The cut-off frequencies, angle of incidence and attenuation are used within the theory to identify operating limitations of passive RFID systems in hollow metal pipes. Source excitations are used to discuss the

characteristics of multi-modal RF propagation. A comprehensive general theory is developed to enumerate the workings of passive RFID systems in circular metal pipes. Analytical evaluations are used to visualize the tags within the metal pipes and to validate the theory presented in this paper. It is shown that passive UHF RFID tags can be read even below the cutoff frequencies of these circular metal pipes when used under the guidance of the general theory. It is also shown that a helical or modified helical tag antenna design would yield high readability rates when impedance matched appropriately to the application specific integrated circuit (ASIC) in the RFID tag.

TABLE OF CONTENTS

LIST OF ILLUSTRATIONS

LIST OF TABLES

CHAPTER 1

INTRODUCTION

There is an increasing amount of interest within the industry for implementation of RFID based systems into various new and emerging applications. In most cases, a theoretical background on fundamental limitations of the technology is highly desirable. Often times using this background, research is conducted to push the limits and boundaries to which these technologies operate by. In this paper we will discuss the ability of RFID systems to function in metal pipes. Currently, high volume of metal pipes in assets will not accommodate passive tags to be located outside these cylindrical designs for various factors including but not limited to the damaging of tags. The inability of tags to be mounted on the outside of these cylindrical metal structures has spurred interesting investigations into the workings of this technology around metals, which is studied thoroughly in this paper. In this technical paper, we will discuss the workings of passive RFID tags inside metal pipes.

1.1 Radio Frequency Identification (RFID) Systems

RFID is an automated identification and data capture technology that has become very popular in many industries around the world. The basic operational principle of this vastly old technology relies on radio frequency (RF) communication and is generally fast and reliable. Examples of industries that have successfully utilized this automated identification and data capture technology are not limited to the service

industries, purchasing and distribution logistics, manufacturing companies and material flow systems. The existence of RFID today derives from the fact that it does not require a line-of sight (LOS) or contact for its communication. This non-LOS capability allows it to challenge the existence of the barcode system and enables for many other applications besides the obvious. Other stumbling blocks of barcodes are due to their low storage capacity and non-existence of re-programmability. RF Identification systems were developed decades ago for the purpose of identifying friends or foes during World War II. The RFID market now belongs to the fastest growing sector of radio technology industry, including mobile phones and cordless telephones (Figure 1.1) [1].

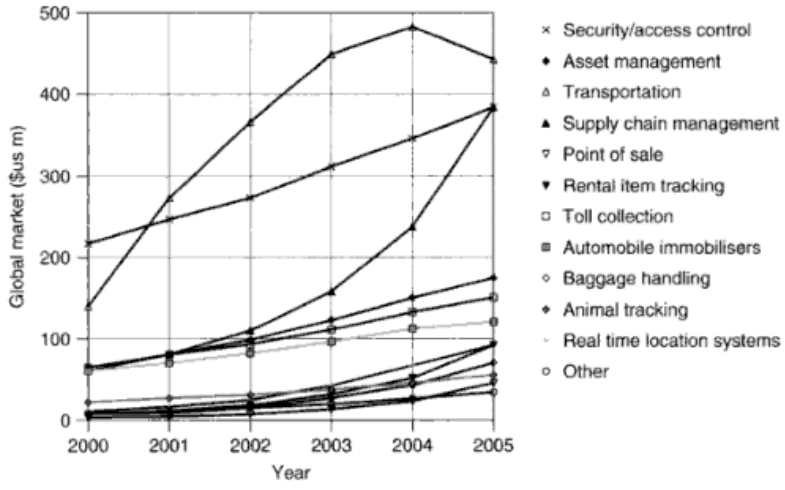

Figure 1.1: Estimated growth of the global market for RFID systems between 2000 and 2005 in million $US [1]

The number of companies actively involved in development and sales RFID systems are constantly growing at a high rate. Therefore global sales of these systems which

exceeded 900 $US million in the year 2000 are predicted to reach or surpass 5000 $US million by the end 2007 [2].

RFID Systems generally consists of three major components namely the reader, transponder (hereon referred to as the tag) and the information system. This categorization is an important starting point for the definition of current RFID Systems. Figure 1.2 depicts a typical RFID system layout. The interrogation of the tag is done by the reader accompanied by an antenna and the relevant information is then conveyed to the information system. The information system typically has a huge amount of data and knowledge, thus making knowledge management a key aspect of RFID systems. It is obvious that different application of the technology would require differing information systems, reader systems as well as tags. It is also important to note that although the reader and tag comprise a significant part of the RFID system, the key to RFID enabling an application lies in the information systems. Many companies in various industries have realized this fact earlier on, and proceeded to successfully introduce RFID into their business plans, while some have struggled to implement this technology successfully vastly due to both the lack in the understanding of physical technology limitations and realization of robust information systems.

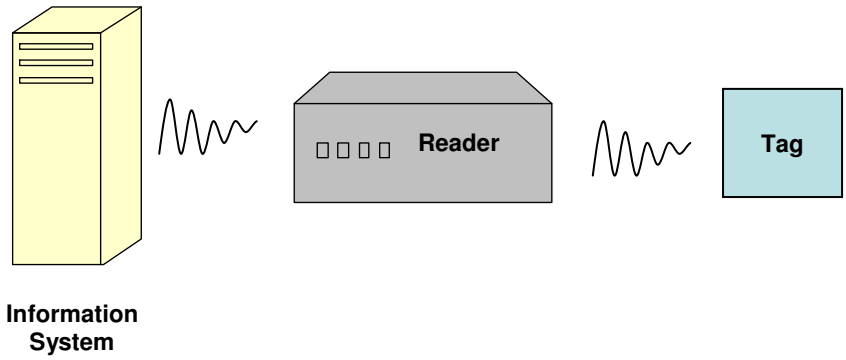

Figure 1.2: RFID System

Typical operations of RFID systems involve a read range (between the tag and the reader) from centimeters up to tens of meters. Current tags can operate up to about 10 meters without a power source (passive tags), while some existing methods allow even larger read ranges. Systems readily available in the market use anywhere from 64 bits to a few kilobits of data transmission and can have identification rates from 50 to 1000 tags per seconds. The prototypical views of RFID Systems today are based on the passive RFID system. In this system, the reader transmits RF energy to power the passive silicon based tags which in essence enables communication to and from the tag. This communication link is possible at any frequencies but is limited to the Industrial, Science and Medical (ISM) frequency bands. In the United States, ISM bands are governed by part 18 of the FCC regulations, while its communication is governed by part 15 of the same body. The various types of RFID systems that exist today allow the globalization or global attack of RFID in the world market while maintaining applicability to highly specific applications and customer needs. Cost of RFID systems,

particularly the tags have been a major issue pertaining to the adoption of the technology and are a key factor in most applications. Globalization of the needs of automated identification and data capture has made RFID into the world leader as an enabling technology for various fields in existence today.

1.2 RFID Reader Systems

The reader is a central module in the realization of any contactless identification system. A software application is used to communicate with the data carrier (tag) through the reader module. This module is therefore a connecting point for the software application to the tag and can be accessed through a set of simple commands. Examples of two general commands are the read and write requests. These are two types of requests that are forwarded to the reader in an attempt to negotiate communication with the tag. As soon as the software application demands the reader module to create the communication link (in this case consider a read request), the reader negotiates these commands by first initiating the link with the tag. The method used frequently for passive tags today involves two simple sets of events. The first event is known as the powering up of the tag. This event is generally known as the tag activation and also includes the execution of the authentication sequence. The second event occurs when the tag replies with the requested data. This is usually called the data transmission from the tag to the reader module. This exemplifies the fact that the readers' main functions are to activate the data carrier (tag), structure the communication sequence with the tag and mediate the communication between the tag and the reader [1].

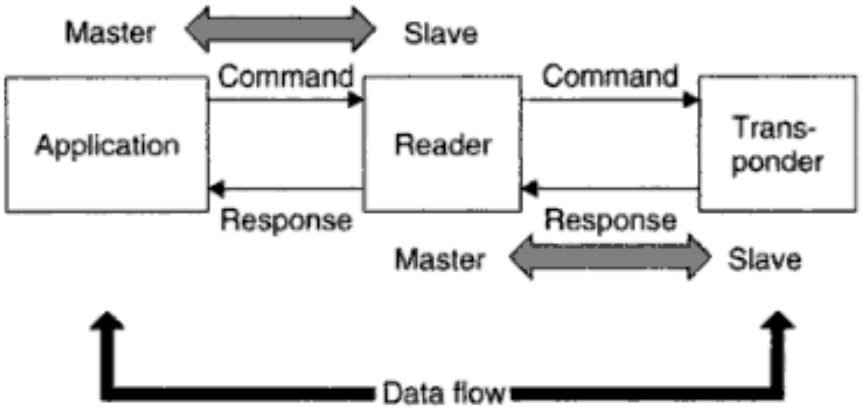

Figure 1.3: Master-slave principle [1]

Another interesting method of classifying the reader and its command hierarchy is to model it using the master-slave principle as shown in Figure 1.3 [1]. This principle displays the events described earlier mainly as commands and responses while maintaining a master-slave relationship between the software application and the reader and also between the reader and the tag. Using this principle, it is practical to describe the read or write commands on the basis of the master-slave relationship. This string of commands and responses shows that the software application acts as a master and sets targets that are accomplished via the reader. This definition implies that the reader is also passive (in its own way), since it never explicitly conduct 'events' without prior approval of the software application. As always, there are major exceptions to this simplistic (yet holistic) view of the reader and a simple example of this is the low-functionality read only tag. As implicitly implied, the reader module must consist of an RF interface, communication control, application subsystem and a network connection.

Some readers have built in antennas although most require external antennas. Finally, most features of the contactless communication process, i.e. making the connection and performing anti-collision and authentication procedures, are handled exclusively by the reader [1].

1.3 RFID Tags

A fundamental difference between the reader module and the tag (or transponder) is the fact that the tag does not consist of the network connection. Unlike the reader, tags do not require network connections since they are designed to work independent of the software application and are never in a position to "chat" with the information system. All that is worth noting here is that only the reader works directly under supervision of the software application. However, tags do consist of all other components as do readers, such as the necessary RF interface, communication control and application subsystem. The radio frequency interface employed here is the antenna and its interface which is obviously required of both the reader and tag. The communication control is also a requirement of both the reader and tag. Although the processes for the communication control are somewhat different for both modules, the simplistic view here is to assume that the results of this complex controls are to negotiate a command which then allows one to muster a response. Finally, the application subsystem of the tag requires the storage of object identifiers (which give potential identification and track/trace ability to the information system) or sensors, whereas the application subsystem in the reader is concentrated in the deciphering of data.

Figure 1.4: Alien Technology Squiggle World Tag

Figure 1.4 is a tag designed by Alien Technologies for operation in the 860 MHz to 960 MHz frequency range and is therefore called a world tag since it allows for its use worldwide. The general design of a tag consist of two physical systems, namely the integrated circuitry on silicon represented by a small odd point generally in the center of Figure 1.4 and the antenna design that dominates the tag size or form factor. Tags generally come in various types of designs (both antenna and the integrated circuit design), however to the naked eye and for practical purposes only the antenna design variations are visible. These differing designs change the characteristics of these tags and their operations. Generally, a specific design is reflective of its radiation and thus gain patterns and contributes to other fundamental requirements such as but not limited to operational frequencies.

RFID tags must as presented earlier have the ability of storing object identifiers and have some higher functionality such as on-tag memory, on-tag sensors and must be equipped for active communication. The on-tag memory in most cases is required for mission-critical information and portable databases (or cache). Another aspect of the tag functionality is in the area of collision, or rather anti-collision. Some tags, have the

ability to execute anti-collision algorithms that reduce the probability for data or communication collisions which reduce the reliability of the link.

1.4 Communication Classification

Currently there exist three categories of tags in the market. They are the passive, semi-passive and active tags. The passive tags are defined as tags that carry out passive communication and have no on-tag power sources. In this case, passive communication exemplifies the modulation of the carrier wave from the reader module in a backscatter mode. The process is fairly simplistic in nature but require highly intelligent designs. Major considerations for this type of communication are the powering of a tag using the carrier wave and then the use of the powered integrated circuitry to modulate the carrier wave to effectively transmit the tags' object identifier. A semi-passive tag would still by definition consist of passive communication but now however have on-tag power sources. Here, the on-tag power source is used to power-up anything but do not participate in the communication itself. Hence the communication in semi-passive tags stay independently passive and the power derived from this on-board power source can be used for various sensor requirements. Already, we can observe the informational richness that comes with the luxury of on-board power sources. The last type of communication classification is the active tag. The active tags participate in active communication and require on-tag power sources. This device is ideally the most rich in terms of sensors and capabilities. Two obvious metrics for comparisons between these classifications are the cost and the richness. Here we see that the passive tags have the least complexities (or richness) but are most affordable

cost wise when compared to any other tags. This is due to the battery (or cells) that generally require more maintenance and replacements, thus higher costs.

Based on the potential direction for the future of RFID, it is widely speculated and reasonable to introduce a new definition of tags based on the power requirements. Electronic tags could potentially be defined as follows [3]:

A. Passive tags, that require no power supply
B. Reader powered active tags
C. Battery powered active tags

The striking differences here are the reclassification of passive tags. The reason for this is the fact that passive tags such as SAW (Surface Acoustic Wave) based RFID tags are essentially a pure form of passive tags that are essentially completely passive as they do not require the charging of capacitors (or cells essentially) such as in IC based RFID tags. The underlying principles of SAW tags using the piezoelectric effect allows for the completely passive operation of the system. Here we ignore these huge implications to the communication classification of RFID tags and stick to the simplistic yet holistic view.

1.5 Passive vs. Active RFID Systems

For most parts, the RFID market concentrates on major differences between the passive and active RFID systems. More importantly, a comparison of their respective advantages and disadvantages are often performed to help the customer generate key concepts about these two different technologies and thus gain insights into the preferred

solution for their specific application. The obvious difference between the passive and active system is that the passive system does not have a battery while the active system does. However, there are other advantages and disadvantages that prove equally pertinent when there is a need to understand many other complexities, such as read range, cost device complexity, functionality and so on. Therefore, it is appropriate to list some of these differences to allow a slightly comprehensive view of both the passive and active systems.

1.5.1 Passive RFID Systems

Today, there is much hype surrounding passive RFID systems. Although, as touched earlier on, the reclassification of communication links could someday morph current passive systems into a new classification called reader powered active systems, it is highly unlikely that there would not be continued interests in current passive systems. In fact, many believe that the current definitions of passive systems are probably a major part of RFID systems in the future (they already are a major part of RFID systems today). On the other hand, there are some who believe that a new classification of purely passive systems could mount a good challenge.

As mentioned before, passive systems imply explicitly the non-existence of batteries. This directly implies that passive systems require no battery changes or replacements, are potentially smaller (or weigh lesser) and are relatively low in cost. Indirectly, passive systems are also less complex (or low in complexity) and thus cannot much functionality (low functionality). Another direct implication of passive systems are their short communication range (read range) when compared to active systems.

This is inherent, given their low power outputs from the tags, since only a backscatter mechanism is implemented. An interesting point not always portrayed when comparing passive to active systems are the obstructions in the environment. Because of lower power levels, a communication link between a passive tag and a reader is highly hindered when there are obstructions in the LOS or surrounding. Most objects act as obstruction and can severely attenuate the signal power levels pumped out by the tag. This obviously reduces the received signal strength (RSS) at the reader and at some point becomes unrecoverable. Although, the obvious choice when considering performance should be the active systems, majority of applications using RFID seem to concentrate solely on passive systems. This is so due to the low costs of passive systems and also the life-time of the system (no battery replacements required).

1.5.2 Active RFID Systems

At this point, it is obvious that the active systems are quite different from their passive counterparts. Some of the key ingredients as enlightened previously are the requirements for battery changes or replacements and the need to conserve energy (to extend battery life and therefore system life time). Another important distinction of the active system is the high cost of these systems owing itself mainly to the high price of batteries. However, nature as always has its ways of balancing itself and similarly active systems have much higher functionality. A direct implication of battery powered systems are the longer communication ranges (read ranges) inherent in the active systems. Putting all together, we seem to realize that passive and active RFID systems do happily co inhibit. Although they seem to compete for either low complexity and

thus low costs or high functionality and long communication ranges, they are both are highly application specific. The applicability of these systems are as expected very selective based on the needs of the application. This is also the fundamental view on RFID as a whole. The technology itself is inherently variable and therefore highly customizable. This variability gives uniqueness that is seldom observed in such physically fundamental technologies. Finally, there exists an important point worth noting regarding the communication range. Realize that there is no bearing on whether the read range is advantageous or conversely disadvantageous to the specific variability that exists in passive as well as active systems. The reason for this is the fact that unlike the previous juncture during the early stages of RFID adoption, communication ranges now have become highly critical in the privacy and security community. Higher read ranges or communication ranges are not just advantageous anymore but could also be disadvantageous. Longer communication ranges promote eavesdropping which is a potentially lethal privacy issue when considering automated identification schemes. Therefore, it is interestingly noted that short communication ranges are now an advantage and disadvantage for passive systems. Similarly, long communication ranges are both an advantage and disadvantage for active systems.

1.6 Performance of RFID Systems

Initially, there exists a tendency to generalize performance as read rate and range (communication range). However, it is quickly discovered by experts in the field of RFID that performance is a complex variable to say the least. Today, read rate and range are only the obvious methods of defining performances of RFID systems. Metrics

that define the performances of RFID systems are currently highly incomplete and lack clear definitions. Some organizations such as the Texas Radio Frequency Innovation and Technology Center are conducting research that could potentially revolutionize a metric format for performance analysis of RFID systems. If these specific performance metrics are created in the future, it would allow for an easier adoption of the technology worldwide as it enables an apple-to-apple comparison of all technologies in existence.

UHF 860MHz – 960MHz

Radio frequency identification is required to operate within the ISM band as mentioned earlier and therefore have specific operable frequencies. The majority of RFID systems today operate within the allocated LF (low frequency), HF (high frequency), UHF (ultra high frequency) and microwave bands. Operations in these bands are specifically detailed in the appropriate FCC (part 15 and 18) regulations. As noted, communication frequencies are classified as [4]:

A. Low Frequency (0-300kHz)
B. High Frequency (3MHz-30MHz)
C. Ultra High Frequency (300MHz-3GHz)
D. Microwave Frequency (>3GHz)

Note that this classification is generally accepted but often seem softer around the edges. For example, a 2.45GHz frequency is often called a microwave frequency. RFID systems are also operated within the ISM bands that have specific frequency allocation. The ISM band allocations for passive RFID systems are 0-135kHz, 13.56MHz,

27.125MHz, 433.92MHz, 869MHz, 915MHz (except in Europe), 2.45GHz, 5.8GHz and 24.125GHz [4]. The RFID market today for most parts has concentrated a lot of effort to adopt the UHF version of the technology. This is done so for quite a few good reasons. The advantages of a general UHF RFID system are [4]:

A. Effectiveness around metals
B. Best available frequencies for long range passive communication
C. Relatively small tag size
D. Smaller antenna sizes
E. Communication Range
F. Good non-LOS (non-line-of-sight)
G. High data rate
H. Controlled read zones

Some other issues with systems generally operating in the UHF band seem to have much bearing on the regulations and signal penetration for conductive or 'lossy' materials. Although UHF systems have good non-LOS ability, this is only guaranteed in ideal environments. In a non-ideal environment with conductive materials such as metals or 'lossy' materials such as water/tissue, the performance of these systems degrade and can show signs of deterioration. Many deployment efforts are hampered because of the lack of understanding of the fundamental theories for the operation of RFID systems. Experts in the field however, can very successfully design a UHF system to work around these environmental conditions and most times are able to

maintain a high level of performance for these UHF systems. Another concern as noted above is the regulatory issues that slow the global effort of UHF systems. Regulations around the world require systems with differing characteristics, mainly in operable frequencies, channels, power and duty cycle [4]. The already growing market for RFID systems will benefit tremendously, if a global effort is able to someday allow for a single regulatory body to set and monitor the regulations for these systems worldwide.

1.7 Tag Performance Dependencies

As related to earlier, the performances of RFID systems are in general relatively complex in nature. These complexities tend to be neglected for various reasons. Often, the performance of a system is measured using the two obvious metrics, read range (communication range) and read (or rather identification) rate. These two metrics are very important in promoting the understanding of a specific system. However, the limitations incurred when using this idealistic and simplistic view can be disastrous, and have often been financially painful for many early adopters. Although a complete metric has yet to be developed, a good start would be to engage into the details regarding read ranges and read rates. To do so successfully, one must understand the factors that govern these two metrics. Some factors that govern the read rates are [4]:

A. Frequencies
B. Number of tags in the field
C. Obstacles in the environment
D. Humidity
E. Temperature

F. RF interference (noise)

G. Tag to reader separation

H. Polarization mismatches

I. Reader identification algorithm

It is important to keep an open mind regarding the above listed issues when considering the read or identification rate. All listed issues bear significant implications on tag performances of RFID systems, particularly for passive systems. Similarly, the factors that govern the read (or communication) rate (including all of the above) are [4]:

A. Tag design and implementation

B. Antenna design

Note that the listed issues are just some of the pertinent issues that must be comprehended to understand the detail pertaining to read range and read rate metrics. There are at least a few more metrics that are very important to RFID systems. These and the two argued earlier must be someday detailed theoretically to allow for an apple-to-apple comparison of RFID systems.

1.8 Antennae Systems

The antenna system adopted by any RFID system is automatically a key area of interests. This is so because it impacts the way the technology works and therefore impacts its performance and hence its applications. Antenna design is actually an interesting part of passive RFID systems today and will remain a vigorous part of the

technology for many decades. When considering passive systems, antenna systems must be designed to accommodate for read performances through key factors such as antenna gain and frequencies. However, the even more intriguing aspect of this field deals with the intelligent design of antennae to allow for high performances around or close to 'lossy' materials and conductive materials. Both tag and reader antenna designs are equally important and some other selection criteria include but are not limited to [4]:

A. Antenna size
B. Polarization
C. Directionality

Besides the above selection criteria, antenna locations for reading zones are often critical to performances of RFID systems.

RFID systems are a revolutionary tool that enables automated identification and data capturing. It is a system invented during World War II for the friend-or-foe identification (IFF) and has since been utilized for various types of identification scheme. RFID based technology have been evolving and have undergone steady growth ever since. Recent innovations allow for the better use of existing and surrounding infrastructures, and have better performances as well as more cost effective designs [4]. Major and critical improvements in costs of RFID systems will generally dominate the adoption criteria for the next few years, while globalization through regulatory bodies will obviously create an even greater potential growth factor for the system worldwide. These factors and other standardization issues involving but not limited to political

concerns with EPC Global and ISO will dominate a majority of the worldwide adoption growth issues for RFID systems in the near future.

1.9 Purpose and Direction

The characteristics of RF propagation as related to passive RFID systems must be studied to reveal the workings in a metal pipe. Similarly, metal pipes must be modeled as an electromagnetic compatible structure that would yield to the fundamental Maxwell laws. With the two most important steps covered, this paper would move ahead and examine the fundamentals of RF propagation in metal pipes using known mathematical special functions such as the Bessel function. These special functions are then used to describe the fundamental limitations of passive RFID systems. Potential solutions to passive RFID systems in metal pipes are presented and further discussions are elaborated.

This paper is organized as follows: a background on the modeling of metal pipes and fundamental electromagnetism is presented in Section 2. Motivation for this topic is demonstrated in Section 3. Mathematical analysis and waveguide engineering is presented in Section 4. The special mathematical function called the Bessel function is introduced in Section 5. Theory and limitations of passive RFID systems in hollow metal pipes are presented in Section 6. A general theoretical solution is presented here. The radiation patterns of RFID tags are simulated comprehensively in Section 7. In Section 8, the proposed general theory solution is discussed and validated. This solution is shown to have an impact on the current state of passive wireless communications in

various finite element structures. Finally, a comprehensive conclusion is provided in Section 9.

CHAPTER 2

BACKGROUND

The obvious choice for modeling metal pipes would be to use a cylindrical or circular waveguide. Waveguides are structures used in guiding EM waves at high frequencies. On applying boundary conditions on the wall of the waveguide, basic formulas are obtained for different modes of operation. Cylindrical waveguides comprise of the three types known as:

A. Metal tube waveguides, hollow or filled with dielectric

B. Dielectric waveguides

C. Coaxial waveguides

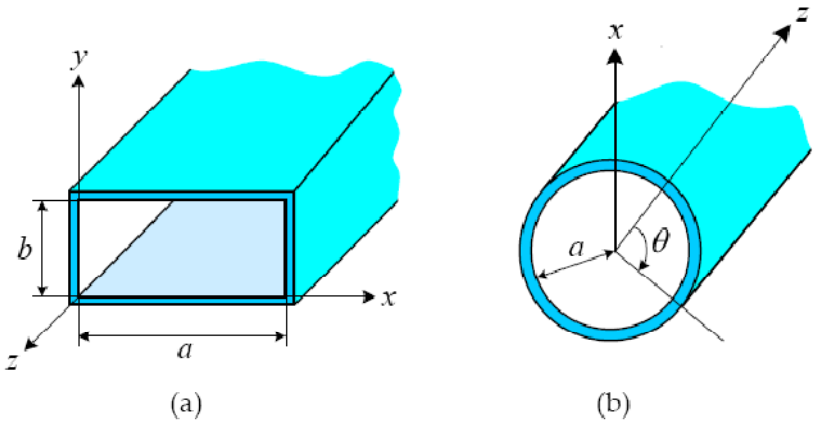

Figure 2.1: Two typical examples of closed waveguides: (a) rectangular waveguide and (b) cylindrical waveguide [5]

Figure 2.1 is a depiction of two common types of waveguides, the rectangular waveguide and the cylindrical waveguide. The key differences are the simple fact that the waveguide dimensions are dictated in (a) by *a* and *b*, whereas in (b) by just *a*. These dimensions cause the RF propagation and modes to be different between the two waveguides. When discussing metal pipes, it is quite easy to see that the cylindrical waveguide is the right choice. In this paper, we will show the mathematics behind cylindrical waveguides, but more importantly the metal tube waveguides, hollow or filled with air.

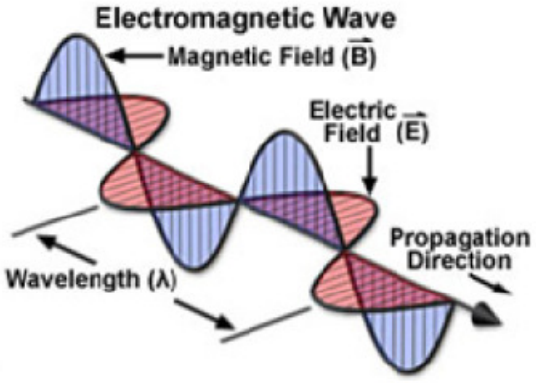

Figure 2.2: Plane electromagnetic wave propagation [6]

Figure 2.2 depicts the plane electromagnetic wave propagation. The electric field and the magnetic field are known to generate each other and behave perpendicular in nature. Both the vectors and propagation direction are strictly perpendicular in nature. These electromagnetic waves must be solved with boundary conditions at the edges of the waveguides using Maxwell or variants thereof to obtain solutions. The boundary conditions are typically represented by the material composition as well as their

interfaces. The solutions (also called modes) to these equations would yield eigenvalues that are direct representations of axial wave velocities in the waveguides. There are two common transverse modes of propagation called the TE (transverse electric) and TM (transverse magnetic) mode, which will be referred to often in this literature. Each propagation mode has an associated propagation constant and cutoff frequency. The dominant mode of operation is the lowest mode possible. It is the mode with the lowest cutoff frequency. There are also two other modes, namely the TEM (transverse electromagnetic) and the HE (hybrid) mode. The four different mode categories as described above are:

A. Transverse electromagnetic (TEM)
B. Transverse electric (TE)
C. Transverse magnetic (TM)
D. Hybrid (HE)

In the transverse electromagnetic (TEM) mode, both the **E** and **H** fields are transverse to the direction of the wave propagation. Therefore $E_Z = 0 = H_z$, resulting in the fact that the TEM modes cannot exist in hollow metallic waveguides. However, the transverse electric (TE) and transverse magnetic (TM) exists freely depending on the characteristics of the wave (wavelength or frequency) and waveguide properties. Hybrid (HE) modes exist in the cylindrical waveguides but present a rather complex problem by itself. The analysis of this mode type is rather dubious and hardly relevant since they are rarely in dominance [6]. Therefore for the purpose of this paper, the HE modes are

not considered. In the section that follows, a clear motivation is presented for the proposed research of understanding the workings of passive RFID systems in metal pipes.

CHAPTER 3

MOTIVATION

The motivation for the characterization of RF propagation in metal pipes stems from the industry's need to track and trace metal pipes in volume using low cost technologies. The case for lost and misplaced metal pipes is staggering and could hurt the bottom line for a company in this tubular industry. Organizations offering metallic products have for a very long time been in much need of a supporting framework such as obtainable by the auto-id technologies. Track and trace capabilities will not only revolutionize the tubular industry, but will also contribute immensely in customer satisfaction as it will give the user tremendous access to the world of information systems. This new world will not only reduce complications and gain customer confidence, but it will also create a very lean industry that would continuously be more and more efficient. Authentication systems powered by a global information system will enable an incredible amount of confidence in the industry, which would allow for a seamless stream of business opportunities. Most major players in this industry are immensely concentrated in the large diameter pipes market, specifically for the oil and gas pipeline projects worldwide. These projects are typically high value projects and therefore any delay, mishandling or wrong shipments could cause a significant impact on profit margins. Similarly, understanding RF propagation in light of passive RFID technologies could someday revolutionize the track and trace of other high valued

metallic objects. Today, most metallic objects produced in the industry with high demand or volume stay away from passive RFID technologies for the simple reasons that the technology lacks a guaranteed solution. A better understanding of the nature of RF propagation and its limitation in view of passive RFID technologies would allow the appropriate industries to recalculate their return-on-investments (ROI) in a more calculated and assured manner. In the following section, the fundamental mathematics behind waveguide engineering is introduced. This section assumes some background in electromagnetism.

CHAPTER 4

MATHEMATICAL ANALYSIS

Considering a straight cylindrical waveguide having an arbitrary cross section and lying along the z-axis, the electric field intensities inside satisfy the following homogenous vector Helmholtz's equation, where **E** is the three dimensional vector phasors [7].

$$\nabla_{tr}^2 \boldsymbol{E} + (\gamma^{-2} + \omega^2 \mu\varepsilon)\boldsymbol{E} = 0 \tag{1}$$

For cylindrical coordinates,

$$\nabla_{tr}^2 = \frac{\partial^2}{\partial r^2} + \frac{1}{r}\frac{\partial}{\partial r} + \frac{1}{r^2}\frac{\partial^2}{\partial \theta^2} \tag{2}$$

Substituting $\boldsymbol{E}_{\boldsymbol{Z}}^{0}(r,\theta) = f(r)g(\theta)$ into the wave equation, dividing by f_g and defining $h^2 = \gamma^{-2} + \omega^2\mu\varepsilon$,

$$\frac{1}{f}\frac{\partial^2 f}{\partial r^2} + \frac{1}{fr}\frac{\partial f}{\partial r} + \frac{1}{gr^2}\frac{\partial^2 g}{\partial \theta^2} + h^2 = 0 \tag{3}$$

This can then be multiplied by r^2 and collected by terms to form,

$$\frac{r}{f}\left[r\frac{d^2f}{dr^2}+\frac{df}{dr}\right]+h^2r^2+\frac{1}{g}\frac{d^2g}{d\theta^2}=0 \tag{4}$$

Recognizing that the terms on the left are only a function of r, that the terms on the right are only a function of θ and that,

$$r\frac{d^2f}{dr^2}+\frac{df}{dr}=\frac{d}{dr}\left(r\frac{df}{dr}\right) \tag{5}$$

We can rewrite the wave equation as,

$$\frac{r}{f}\frac{d}{dr}\left(r\frac{df}{dr}\right)+h^2r^2=-\frac{1}{g}\frac{d^2g}{d\theta^2}=n^2 \tag{6}$$

Where n is an integer constant requirement from the equation for $g(\theta)$ and is required to be continues or periodic at 2π. Examining the wave equation,

$$-\frac{1}{g}\frac{d^2g}{d\theta^2}=n^2 \tag{7}$$

$$\frac{d^2g}{d\theta^2}+n^2g=0 \tag{8}$$

which has the general solution,

$$g(\theta) = C_1 \cos(n\theta) + C_2 \sin(n\theta) \tag{9}$$

that we can rewrite as,

$$\frac{d^2 f}{dr^2} + \frac{1}{r}\frac{df}{dr} + \left(h^2 - \frac{n^2}{r^2}\right) f = 0 \tag{10}$$

This is the famous Bessel's function, which has the general solution [7],

$$f(r) = C_3 J_n(hr) + C_4 Y_n(hr) \tag{11}$$

where, J_n is the n-th order Bessel function of the first kind and, Y_n is the n-th order Bessel function of the second kind, both of which functions and properties are very well known. For cylindrical waveguides, finite fields at all points are highly desirable, which translate to no changes within the guide and therefore all forms of Y_n are rejected since,

$$\lim_{r \to 0} Y_n(r) = -\infty \tag{12}$$

CHAPTER 5

THE BESSEL FUNCTION

Figure 2.3 carefully depicts the Bessel function for the cylindrical waveguide problem. Notice that these functions behave very much alike to the $\sin x/x$ function. They start at 1 or 0 and decrease as u increases. However, the period changes as r changes. Rarely, will there be a need for higher order Bessel functions in the case of cylindrical waveguides. The two main types of Bessel functions are typically referred to the first kind and second kind respectively. These functions are used often when solving electromagnetic problems in cylindrical or spherical coordinates using the Helmholtz Equation or Laplace's Equation. Bessel functions of the first kind are functions that have finite initial conditions and are obtained by solving the differential equations for non-negative orders [8, 9]. Figure 2.3 below is a plot of the Bessel function of the first kind, where the colors denote higher order functions.

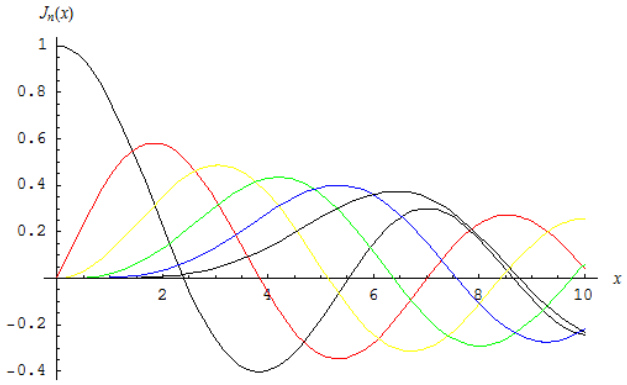

Figure 5.1: Bessel function of the first kind

Similarly, the Bessel functions of the second kind are solutions to the differential equations with a singularity for its origin instead. This function with a negative infinite singularity is sometimes called the Neumann function and is depicted in Figure 5.2 below.

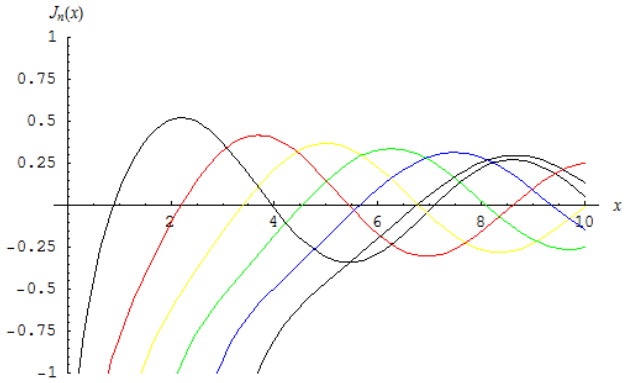

Figure 5.2: Bessel function of the second kind

For the purpose of the metal pipe analysis, the Bessel function of the first kind is highly applicable and is used throughout this paper. In an attempt to understand the

details regarding this special type of function, a visualization of the complex and contour plots for the Bessel function is studied closely. Figure 5.3 and 5.4 depicts the complex 3D and contour plots of the Bessel function of the first kind at the 0^{th} order.

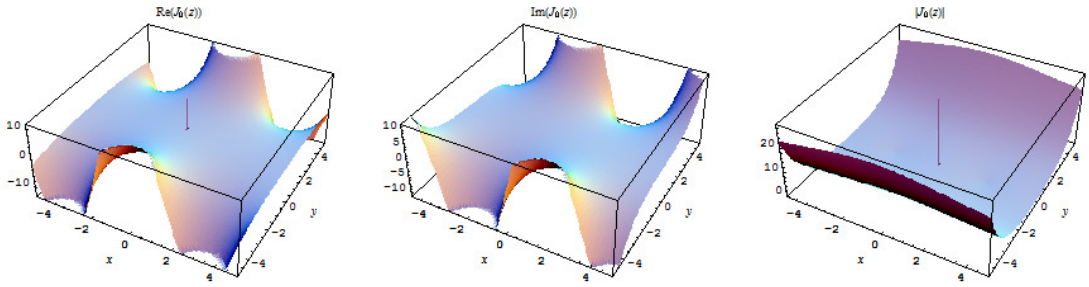

Figure 5.3: Complex 3D plots of the Bessel function of the first kind with n=0

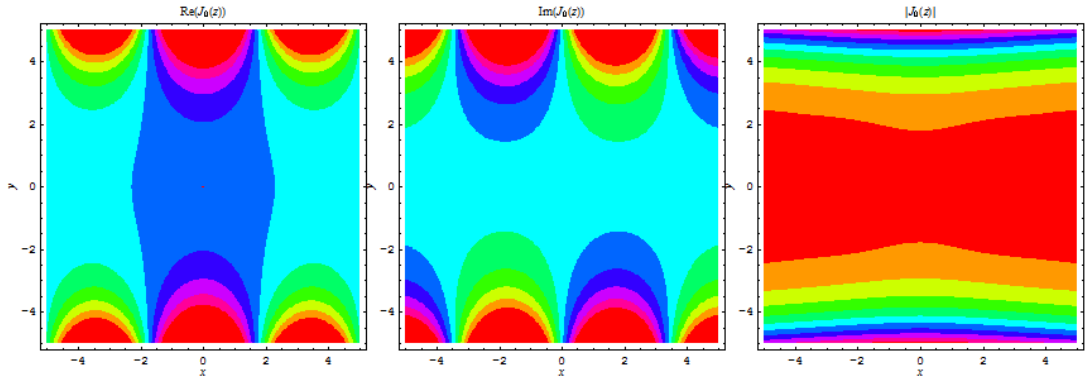

Figure 5.4: Contour plots of the Bessel function of the first kind with n=0

Notice that the imaginary and real plots are somewhat phase shifted and are otherwise similar in most perspective. The Bessel functions are roughly oscillating sin or cosine functions that decay exponentially but generally have non-periodical roots. Figure 5.5 and 5.6 depict the Bessel functions of the first kind at the 10^{th} order, where

the number of oscillatory functions increase as the order of the function increases. This is simply the nature of this mathematical model and is used successfully for characterizing electromagnetic waves in cylindrical metal pipes. The mathematical analysis in this paper assumes a summation of all orders of Bessel functions that exist. Although this is a good practice, the specific nature of each environment is typically different and requires alternate order deductions. These deductions are outside the scope of this paper and will be tackled in later publications.

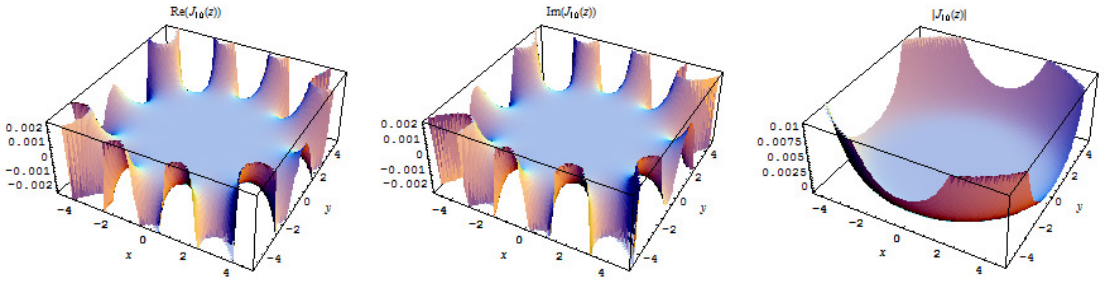

Figure 5.5: Complex 3D plots of the Bessel function of the first kind with n=10

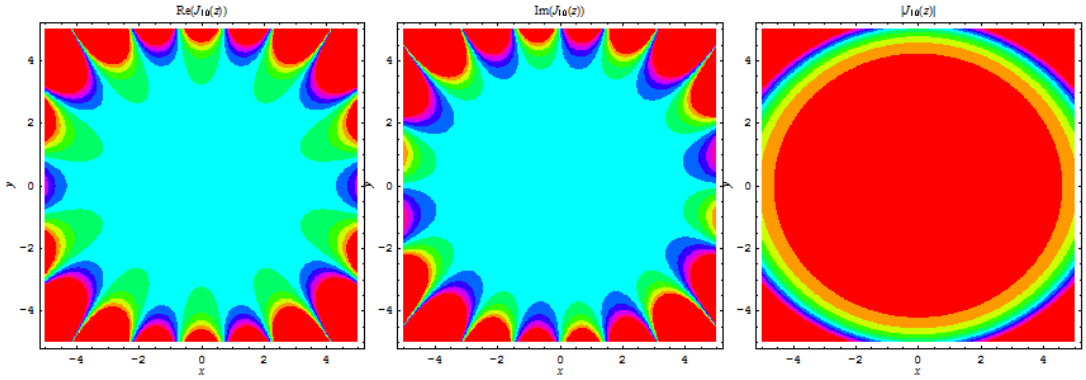

Figure 5.6: Contour plots of the Bessel function of the first kind with n=10

Table 5.1 below indicates the values for u at $J_n = 0$. This table denotes the roots to the Bessel function of the first kind. These roots are recorded for the first three orders of the function as higher orders are typically non-pertinent when studied under the context of electromagnetic modal analysis in metal pipes [10].

Table 5.1: Roots of the Bessel function of the first kind for the transverse electric mode

	$J_0(u)$	$J_1(u)$	$J_2(u)$
	2.405	3.832	5.136
u	5.520	7.013	8.417
	8.654	10.173	11.620

Using the knowledge and information provided above, the general solution for the electric field for a given mode at a specific spherical radius and angle is derived. This general solution can be very easily shown to be:

$$E_Z^0(r,\theta) = C_3 J_n(hr)[C_1 \cos(n\theta) + C_2 \sin(n\theta)] \tag{13}$$

Since we expect the solutions to be independent of the origin, the general solution can be simplified to get,

$$E_Z^0(r,\theta) = C_n J_n(hr) \cos(n\theta) \tag{14}$$

At the metal wall, $E = 0$ and therefore $J_n(hr) = 0$. Since $t_{nl} = u$, we get the equation,

$$h_{TM_{nl}} = \frac{t_{nl}}{r} = \frac{t_{nl}}{a} \tag{15}$$

where n is the number of circumferential variations and l is the number of radial variations. The propagation constant is therefore [6, 7],

$$\bar{\beta}_{TM_{nl}} = \left[\omega^2 \mu\varepsilon - \left(\frac{t_{nl}}{a}\right)^2\right]^{1/2} \tag{16}$$

where propagation only occurs for $f > f_{C_{TM_{nl}}}$. This then gives,

$$f_{C_{TM_{nl}}} = \frac{t_{nl}}{2\pi a\sqrt{\mu\varepsilon}} \tag{17}$$

Where the lowest cutoff frequency is $t_{01} = 2.405$ which makes TM_{01} the transverse magnetic mode with the lowest cutoff frequency. The field components for the circular TM_{nl} modes are [6, 7],

$$E_Z = C_n J_n\left(\frac{t_{nl}}{a} r\right) \cos(n\theta) e^{-j\bar{\beta}_{nl} Z} \tag{18}$$

$$E_r = -\frac{ja\bar{\beta}_{TM_{nl}}}{t_{nl}} C_n J_n'\left(\frac{t_{nl}}{a} r\right) \cos(n\theta) e^{-j\bar{\beta}_{nl} Z} \tag{19}$$

$$E_\theta = \frac{ja^2 n\bar{\beta}_{TM_{nl}}}{t_{nl}^2 r} C_n J_n\left(\frac{t_{nl}}{a} r\right) \sin(n\theta)\, e^{-j\bar{\beta}_{nl} Z} \tag{20}$$

$$H_r = -\frac{j\omega\varepsilon n a^2}{t_{nl}^2 r} C_n J_n\left(\frac{t_{nl}}{a} r\right) \sin(n\theta)\, e^{-j\bar{\beta}_{nl} Z} \tag{21}$$

$$H_\theta = -\frac{j\omega\varepsilon a}{t_{nl}} C_n J_n'\left(\frac{t_{nl}}{a} r\right) \cos(n\theta) e^{-j\bar{\beta}_{nl} Z} \tag{22}$$

$$H_Z = 0 \tag{23}$$

The transverse electric modes are calculated similarly. The only difference that exists is that now $E_Z = 0$. The eigenvalues of the solution come from the zeroes of J_n' instead of J_n, which are called s_{nl}, such that

$$\bar{\beta}_{TE_{nl}} = \left[\omega^2 \mu\varepsilon - \left(\frac{s_{nl}}{a}\right)^2\right]^{1/2} \tag{24}$$

$$f_{C_{TE_{nl}}} = \frac{s_{nl}}{2\pi a\sqrt{\mu\varepsilon}} \tag{25}$$

Table 5.2 identifies the roots of J_n', similar to Table 5.1 for the transverse magnetic mode.

Table 5.2: Roots of the Bessel function of the first kind for the transverse magnetic mode

	$J_0'(u)$	$J_1'(u)$	$J_2'(u)$
	3.832	1.841	3.054
u	7.016	5.331	6.706
	10.173	8.536	9.969
	13.324	11.706	13.170

It is very important to point out that $s_{11} = 1.841$ is the value of the lowest zero and therefore gives TE_{11} the lowest cutoff frequency. Therefore, similarly the complete field components for the circular TE_{nl} modes are [6, 7],

$$H_Z = C_n J_n\left(\frac{s_{nl}}{a}r\right)\cos(n\theta)e^{-j\bar{\beta}_{nl}Z} \tag{26}$$

$$H_r = -\frac{ja\bar{\beta}_{TE_{nl}}}{s_{nl}} C_n J_n'\left(\frac{s_{nl}}{a}r\right)\cos(n\theta)e^{-j\bar{\beta}_{nl}Z} \tag{27}$$

$$H_\theta = \frac{ja^2 n\bar{\beta}_{TE_{nl}}}{s_{nl}^2 r} C_n J_n\left(\frac{s_{nl}}{a}r\right)\sin(n\theta)\, e^{-j\bar{\beta}_{nl}Z} \tag{28}$$

$$E_r = \frac{j\omega\mu n a^2}{s_{nl}^2 r} C_n J_n\left(\frac{s_{nl}}{a}r\right)\sin(n\theta)\, e^{-j\bar{\beta}_{nl}Z} \tag{29}$$

$$E_\theta = -\frac{j\omega\mu a}{s_{nl}} C_n J_n'\left(\frac{s_{nl}}{a} r\right) \cos(n\theta) e^{-j\bar{\beta}_{nl} Z} \tag{30}$$

$$E_Z = 0 \tag{31}$$

Combining both results for the transverse magnetic and transverse electric, a table of the existing modes can be generated as given in Table 6.1. Notice that the TE_{11} mode has the lowest cutoff frequency of all the modes and therefore is known as the dominant mode. If the chosen wavelength λ is to reside between

$$\lambda_{C_{TE_{11}}} = \frac{2\pi a}{1.841} = 3.41a \tag{32}$$

$$\lambda_{C_{TM_{01}}} = \frac{2\pi a}{2.405} = 2.61a \tag{33}$$

then only the TE_{11} mode will be allowed to propagate. It is important to point out that single mode propagation is highly desirable since it will allow maximum power transmission [6, 7, 8, 9].

CHAPTER 6

THEORY AND LIMITATIONS OF PASSIVE RFID SYSTEMS IN HOLLOW METAL PIPES

Passive RFID systems as related to earlier, are a very interesting technology to be studied with structures such as metal pipes. The major reasons cited here are based on the simple reasons that it is an energy harvesting technology utilizing backscatter for communication. Passive RFID systems and metal pipes are also an interesting mix because of the physical and electromagnetic wave propagation constraints as defined by metal pipes. The three major factors contributing to the limitations of passive RFID in metal pipes are as listed below:

A. Cutoff frequencies as dictated by the diameter of the metal pipe
B. Angle of incidence of the plane waves with the surface opening of the metal pipe
C. Attenuation of the propagated waves
    a. For the operational modes specific to internal propagation
    b. For the external propagation, i.e.: outside the metal pipe

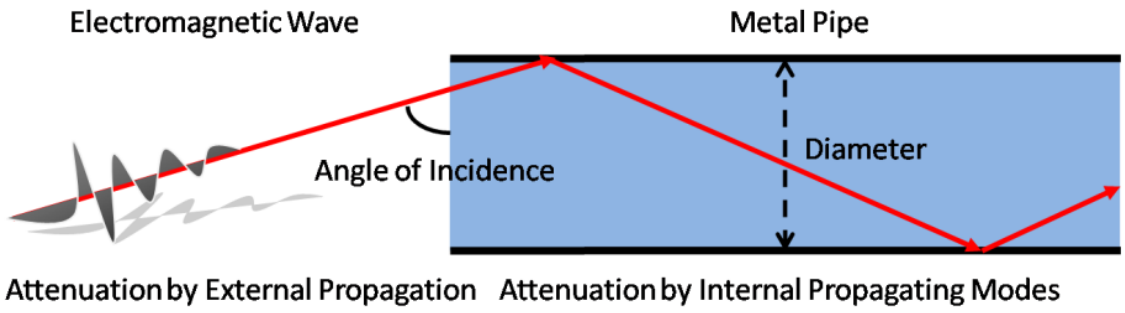

Figure 6.1: Limiting parameters for passive RFID systems in metal pipes

Figure 6.1 depicts the parameters involved in the major limitations as listed above. The total attenuation is broken down into two parts to describe the attenuation caused by external propagation of the waves in free space and the attenuation of the propagating modes in the metal pipe.

$$\alpha_T = \alpha_E + \alpha_I \tag{34}$$

where α_T, α_E, α_I are the total attenuation of the system, attenuation caused by the external propagation and attenuation caused by the internal propagating modes respectively. In the following sections, the details of these limitations pertaining to passive RFID systems as described above are explored. This exploration will include the attenuation, angle of incidence and cutoff frequencies as justified by the diameter and other environmental constants.

6.1 Cutoff Frequencies in Metal Pipes

There exist a fundamental difference between waveguide designs and the problem at hand. Recall that waveguide designs are scenarios when a designer picks a dimension and builds the waveguide. These dimensions are in practice chosen such that the number of modes propagating is limited to either one in best case or limited to very few in some cases. This is done on the premise mentioned above to allow maximum power transmission. It is possible to design such a system given the designer knows the desired frequency and has the ability to pick the dimensions. RFID in metal pipes pose a somewhat different problem since the number of pipes are generally large in volume and have various diameters associated with them. Assuming for example, a UHF RFID system where the frequency and wavelengths are well known. From the previous section, it is obvious that having tags in different pipes (having different dimensions) will enable different types of wave propagation modes in these pipes. If the pipes are sufficiently small in diameter, it is obvious from Section 5 that there might not exist any modes of operation therefore the power transmitted is highly negligible or effectively zero. In this case the RFID tag inside the pipe will be unable to function. The second case is when the diameter of the pipes is within the range, where a single transverse electric mode is allowed to propagate that the power transmitted is very high and not attenuated very much. In the third case the diameter of the pipes are too large and many modes are allowed to propagate and therefore as mentioned before, the power transmitted reduces appropriately.

The three cases are:

A. $f < f_C$: non-propagating waves.

B. $f_{C_{TE_{11}}} < f < f_{C_{TM_{01}}}$: single TE_{11} propagating mode.

C. $f > f_{C_{TM_{01}}}$: power transmission decreases appropriately by the number of operating modes.

Table 6.1: Transverse electric and magnetic components from Equation 35 to 38

TE	**s_{nl}**	**a/λ_C**	**f_C/f_{CTE11}**	**TM**	**t_{nl}**	**a/λ_C**	**f_C/f_{CTE11}**
TE_{12}	5.331	0.8484557	2.8957089	TM_{02}	5.52	0.878536	2.9983705
TE_{22}	6.706	1.0672939	3.6425856	TM_{12}	7.013	1.1161546	3.8093427
TE_{02}	7.016	1.116632	3.8109723	TM_{22}	8.417	1.3396083	4.5719718
TE_{13}	8.536	1.3585477	4.6366105	TM_{03}	8.654	1.377328	4.7007061
TE_{23}	9.969	1.586617	5.4149919	TM_{14}	10.174	1.6192438	5.5263444
TE_{03}	10.173	1.6190846	5.5258012	TM_{24}	11.62	1.849382	6.3117871
TE_{14}	11.706	1.8630693	6.3585008				
TE_{24}	13.17	2.0960724	7.1537208				
TE_{04}	13.324	2.1205823	7.237371				

Using Equation 25 to describe the required transverse electric modes and Equation 17 to describe the transverse magnetic modes, the equations below are generated.

$$\frac{a}{\lambda_{C_{TE_{nl}}}} = \frac{s_{nl}}{2\pi} \tag{35}$$

$$\frac{f_{C_{TE_{nl}}}}{f_{C_{TE_{11}}}} = \frac{s_{nl}}{1.841} \tag{36}$$

$$\frac{a}{\lambda_{C_{TM_{nl}}}} = \frac{t_{nl}}{2\pi} \tag{37}$$

$$\frac{f_{C_{TM_{nl}}}}{f_{C_{TE_{11}}}} = \frac{t_{nl}}{1.841} \tag{38}$$

Similarly using the Equations above, Table 6.1 and Figures 6.2 and 6.3 are generated,

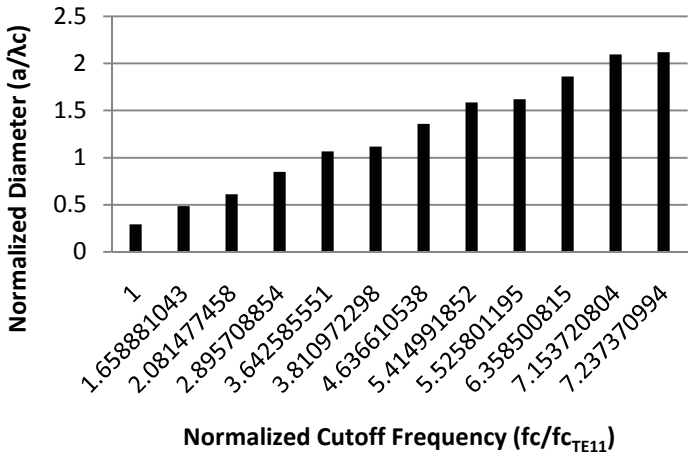

Figure 6.2: Transverse electric modes as generated from table 6.1

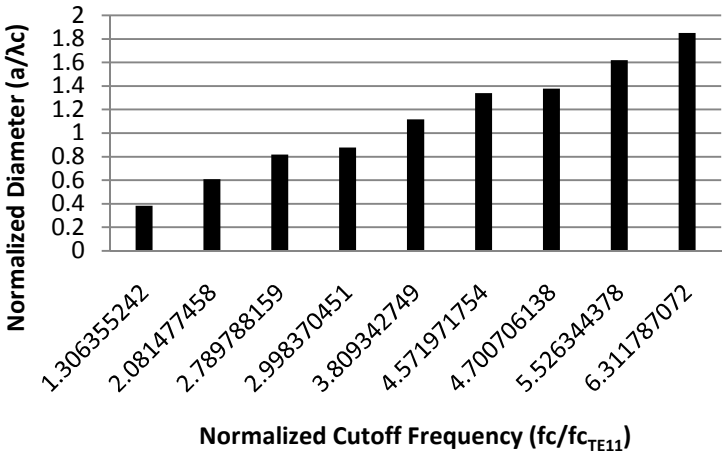

Figure 6.3: Transverse magnetic modes as generated from Table 6.1

Analyzing Figures 6.2 and 6.3, it is easily concluded that there exist a trend when comparing the normalized diameter against the normalized cutoff frequency. A linear curve fitted on these figures yield the following sets of equations:

$$\frac{a}{\lambda_{C_{TE_{nl}}}} = 0.171\left(\frac{f_{C_{TE_{nl}}}}{f_{C_{TE_{11}}}}\right) + 0.141 \tag{39}$$

$$\frac{a}{\lambda_{C_{TM_{nl}}}} = 0.174\left(\frac{f_{C_{TM_{nl}}}}{f_{C_{TE_{11}}}}\right) + 0.237 \tag{40}$$

Using the Equations 39 and 40, a simplified generalization can be made using an averaging mechanism to achieve the equation as noted below.

$$f_{C_{nl}} = \left(\frac{\{s_{nl}, t_{nl}\}}{2\pi} - 0.189\right)\frac{f_{C_{TE_{11}}}}{0.1725} \quad (41)$$

Given the explanation above regarding cutoff frequencies and modes propagating in the metal pipe, there exists a need to put these justifications into context. This is required to give a level of visualization into the propagating modes as well as their causal effects to the RFID tag in the metal pipe. In order to proceed with this visualization, the attenuation of the waves in their respective propagating modes must be analyzed. In the following section, these attenuation factors are studied to reveal a generalized solution for metal pipes.

6.2 Attenuation of the System

The substantial parts addressed in this paper are the attenuation of the system from the exterior as well as interior of the metal pipe. A comprehensive theory of ray based attenuation would allow an extended idea on the power received at a tag in metal pipes. This is indeed a key requirement when analyzing a passive RFID system in an electromagnetic structure such as the metal pipe. The following sections would discuss the attenuation and wave propagation inside and outside metal pipes.

6.2.1 Quantitative Analysis of Path Loss

There are various ways to model the path loss associated with a passive RFID system. These models traditionally use micro-cell environments in an attempt to find a suitable process and theory [11, 15]. Considering metal pipes do complicate the subject but does not significantly alter the propagation phenomenon. In needing to be as accurate as possible, the path loss is considered only for the externally propagating

waves. This would neglect free space losses within the metal pipe which would further complicate matters. The method used in this paper is similar to that employed by [16]. This method enables the simplistic propagation path loss measurements using a minimalistic ray approach for passive RFID systems. The dual slope model used by this method is a generalized approach for predicting the received signal strength using the two ray model [13].

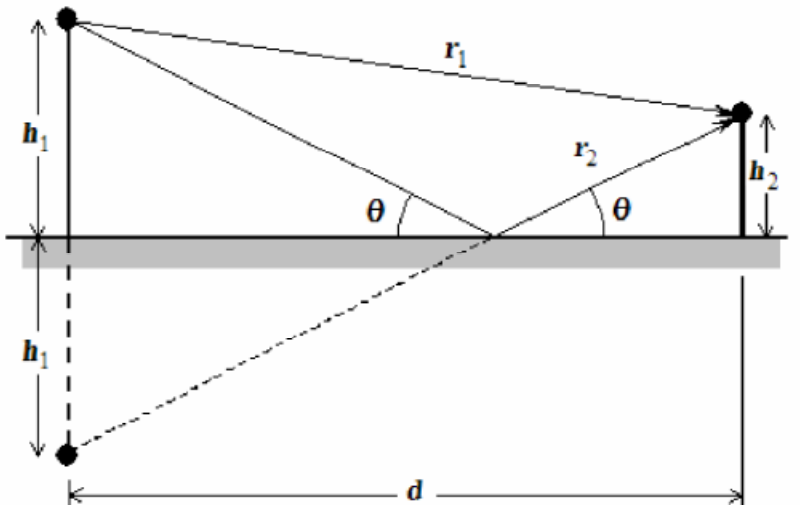

Figure 6.4: The Two Ray Model [16]

Figure 6.4 depicts the two ray model, where r_1 is the direct ray and r_2 is a multi-path ray. The received signal strength at the receiver in the dual slope model is expressed by a modified version of the Friis formula and is shown in Equation 42 [13].

$$P_r = 10\log_{10}\left[\left(\frac{\lambda}{4p}\right)^2 G_t G_r P_t p \frac{1}{r^N} \frac{1}{\left(1+\frac{r}{R_o}\right)^{N_B-2}}\right] \quad (42)$$

P_r = received power

P_t = transmitted power

G_r = reader antenna gain

G_t = tag antenna gain

λ = wavelength

p = polarization mismatch

N = variation of power before the breakpoint

N_B = increased signal loss beyond the breakpoint

R_o = breakpoint distance (Equation 43)

r = distance d as noted in Figure 6.4

$$R_o = \frac{4h_1h_2}{\lambda} \tag{43}$$

h_2 = height of the point of intersect between surface plane of metal pipe and r_1 or r_2

h_1 = reader antenna height above the surface

It is assumed that both the antennas are impedance matched for Equation 42 to be valid and accurate [16]. The values chosen for a typical UHF passive RFID system is indicated below. The unknown variables in the system is assumed to be the height of the point of intersect, h_2 and the distance, d or r.

P_t = 20dBm

G_r = 18dBi

G_t = 1dBi

$\lambda = c/f$, where c is the speed of light ($3.0 \times 10^8 m/s$) and f is the frequency ($915MHz$)

p = 1.0

N = 2.0

N_B = 4.0

R_o = 55.2m

h_1 = 1m

Figure 6.5 is a plot depicting Equations 42 and 43 using the parameters provided above and for the metal pipe (parallel to ground surface) height of 1m above the ground. These values are highly typical for a passive UHF RFID system. Notice that the plot is logarithmic in nature and intersects 0dB at approximately 2 metres away from the reader.

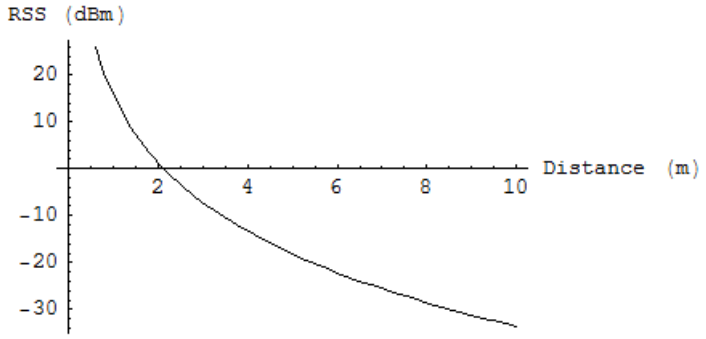

Figure 6.5: Received signal strength at the tag (dBm) vs. distance (m) with h_2=1m

Similarly, using Equations 42 and 43, a plot is generated in Figure 6.6 to depict the results from Figure 6.7 above for all cases of the metal pipe height up to 10 meters. This plot is generated with the reader system located 5 meters above the ground surface. Notice that the rate of decrease for the RSS towards the ground is slower than the rate of increase as the metal pipe divulges away from the ground surface. This is a phenomenon easily quantified when incorporating the two ray model in Figure 6.4.

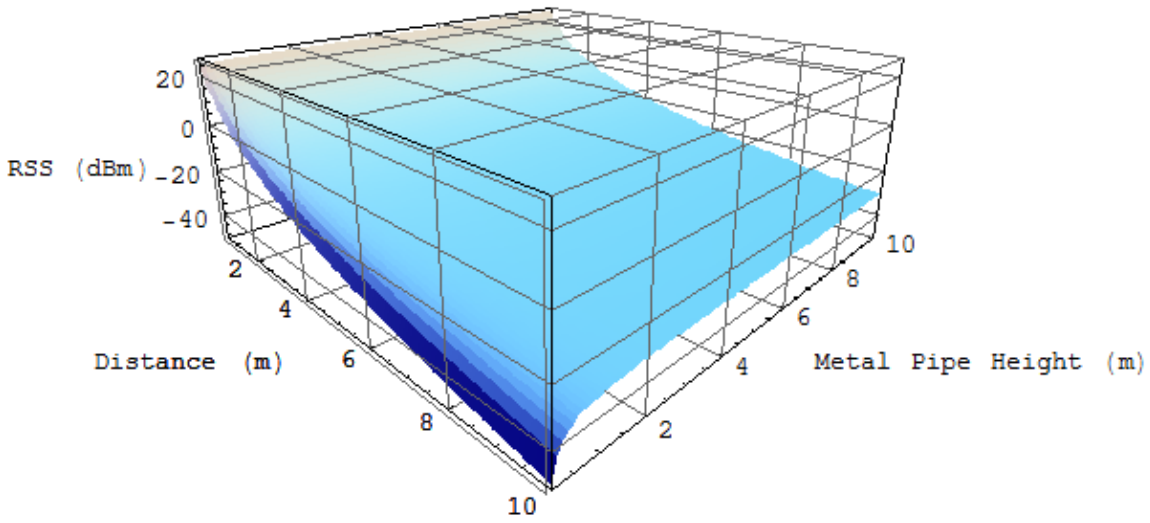

Figure 6.6: Received signal strength at tag vs. distance (m) and height (m) of the metal pipe

In the following section, a quantitative analysis of internal attenuation is derived. Here it is shown that the fundamental modes of propagation play a crucial role again. This role will be exemplified and is shown to have an impact on any potential unified theory proposed in this field. The results of Sections *6.2.1* and *6.2.2* would be the main justifications behind the theory of attenuation in metal pipes.

6.2.2 Quantitative Analysis of Internal Attenuation

Attenuation of electromagnetic waves within the metal pipe is dependent on the propagation mode that exits and is considered to only exist for electromagnetic waves above the cutoff frequency. Within these modal limits, there are two definite boundaries for the attenuation, namely the transverse electric and transverse magnetic modes. Using these definitions and equations leading up to Equation 38, it is found that attenuation for the electromagnetic waves in metal pipes are well explained in the following equations.

$$\alpha_{C_{TM_{nl}}} = \frac{R_s}{a\eta}\left[1 - \left(\frac{f_{C_{TM_{nl}}}}{f}\right)^2\right]^{-\frac{1}{2}}, f > f_{C_{TM_{nl}}} \tag{44}$$

$$\alpha_{C_{TE_{nl}}} = \frac{R_s}{a\eta}\left[1 - \left(\frac{f_{C_{TE_{nl}}}}{f}\right)^2\right]^{-\frac{1}{2}}\left[\left(\frac{f_{C_{TE_{nl}}}}{f}\right)^2 + \frac{n^2}{s_{nl}^2 - n^2}\right], f > f_{C_{TE_{nl}}} \tag{45}$$

$$R_s = \frac{1}{\sigma_c f} = \sqrt{\frac{\pi f \mu}{\sigma_c}}, \sigma_c \approx 10^7 \tag{46}$$

$$\eta = \sqrt{\frac{\mu}{\varepsilon}} \tag{47}$$

Given Equation 44 through Equation 47, the attenuation in metal pipes can be deduced. Equations 48 and 49 are complete representations of the propagation losses in metal

pipes as discovered from the attenuations discussed. These equations are converted to decibel format and take into account the entirety of the constraints as set by metal pipes as well as the propagation path or path travelled.

$$P_{loss_{TM_{nl}}} = \frac{20R_s}{da\eta \ln 10}\left[1 - \left(\frac{f_{C_{TM_{nl}}}}{f}\right)^2\right]^{-\frac{1}{2}} \quad (48)$$

$$P_{loss_{TE_{nl}}} = \frac{20R_s}{da\eta \ln 10}\left[1 - \left(\frac{f_{C_{TE_{nl}}}}{f}\right)^2\right]^{-\frac{1}{2}}\left[\left(\frac{f_{C_{TE_{nl}}}}{f}\right)^2 + \frac{n^2}{s_{nl}^2 - n^2}\right] \quad (49)$$

$$P_L = P_{loss} = \sum_0^{nl}\left\{P_{loss_{TE_{nl}}} + P_{loss_{TM_{nl}}}\right\} \quad (50)$$

Equation 50 represents the power loss for all the modes in a given metal pipe. This equation is derived with the propagation path of the wave in the metal pipe and the diameter of the metal pipe, as strong dependents. Therefore, Equation 50 is rewritten as Equation 51.

$$P_L(d) = \sum_{a=\frac{x_{nl}}{2\pi f_c\sqrt{\mu\varepsilon}}}^{0}\left\{P_{loss_{TE_{nl}}}(d) + P_{loss_{TM_{nl}}}(d)\right\} \quad (51)$$

In the following section, the propagation losses for the electromagnetic waves in metal pipes are combined with the path losses for the general free space propagating wave.

These two concepts are united to reveal a partial solution to the general theory of passive RFID systems in metal pipes.

6.2.3 Theory of Attenuation

Given the concepts related to in the previous sections it is clear that a theory of attenuation for the entire metal pipe system would represent both the internal and external power losses. This theory would be a linear solution and represent the problem as consisting of a single metal pipe. Using the knowledge gathered thus far, Equation 52 below clearly justifies the general solution.

$$P_{r_T} = f(P_r, P_L) \tag{52}$$

In an attempt to reason a proper allocation for the internal power loss, notice that the transmitted power of the reader is very well suited. Here the transmitted power of the reader can be used by subtracting the internal power losses first. This creates a self soluble theory that is shown to be extensible and yet linear in fashion. The equations below display how this extension leads to the solution of the attenuation in metal pipes.

$$P_{t_T} = P_t - P_{loss} = P_t - P_L \tag{53}$$

$$P_{r_T} = P_r\left(P_{t_T}\right) \; or \; P_{r_T} = P_r(P_L) \tag{54}$$

$$P_{r_T} = 10\log_{10}\left[\left(\frac{\lambda}{4p}\right)^2 G_t G_r \left[P_t - \sum_0^{nl}\left\{P_{loss_{TE_{nl}}} + P_{loss_{TM_{nl}}}\right\}\right] p\frac{1}{r^N}\frac{1}{\left(1+\frac{r}{R_0}\right)^{N_B-2}}\right] (55)$$

Equation 55 is a general representation of the scenario as described earlier. This 2-dimensional case is easily solvable in a numerical fashion when using Equations 43, 48, 49 and 55 simultaneously. In a 3-dimensional scenario, the general solution as described above will not yield the correct solutions since the RFID tag and reader system are rarely on the line of sight (LOS) of each other. To tackle this issue, a new system that takes into account the angle of incidence must exist. This system must use the angle of incidence as a way to shape the power transmitted to the tag and allow an accurate measurement or prediction of the power losses suffered by the entire system. In the following section, the angle of incidence of the readers' LOS is studied.

6.3 Angle of Incidence of the Propagating Wave on the Open Surface of the Metal Pipe

The purpose of modeling the viewing angle of the metal pipe is to determine the appropriate maximum amount of energy allowed to permeate through the metal pipe. This enables an accurate estimation of the power received by the RFID tag in the metal pipe when present in a 3-dimensional environment. In these environments, the reader and tag do not necessarily have a LOS view of each other and therefore must be corrected appropriately in the theoretical equations as depicted in the previous sections. Metal pipes or similar cylindrical structures have surfaces resembling circles when viewed from top (90°). However, when viewed at other angles, the surface area of these

structures tends to seem ellipsoidal in nature. This is caused purely by the viewing angle of the structure and requires a new method of modeling.

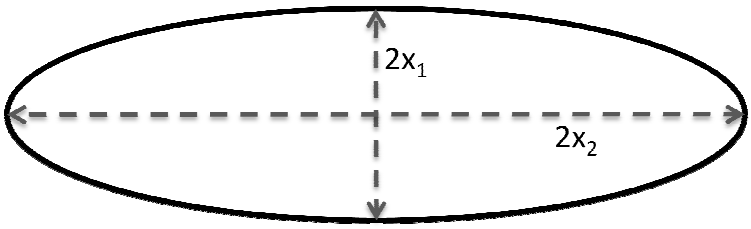

Figure 6.7: The ellipse as perceived from non-LOS angles

The surface area of an ellipse is defined by Equation 56. It clear that the surface area of the circle is equal to the surface area of the ellipse for $x_1 = x_2$.

$$A_e = \pi r^2 = \pi x_1 x_2 \tag{56}$$

Another important perspective is the variance of the perceived surface area of the metal pipe as compared to the angle of incidence. This is a good indication of the characteristics of the propagation theory. The equation below explains the characteristic of the perceived radius, where a is the actual radius and a' is the perceived radius of the metal pipe.

$$a' = a \sin\theta \tag{57}$$

Using Equation 57, the perceived surface area of the metal pipe when compared against the angle of incidence can be calculated.

$$A_e = \pi x_1 x_2 = \pi a' x_2 = \pi a \sin\theta \, x_1 \tag{58}$$

Figure 6.8 depicts the scenario where the angle of incidence changes as the reader moves away from LOS with the tag in the metal pipe. This figure shows the change in perceived surface area of the metal pipe. Notice that the maximum perceived surface area at LOS is $\pi x_1 x_2$.

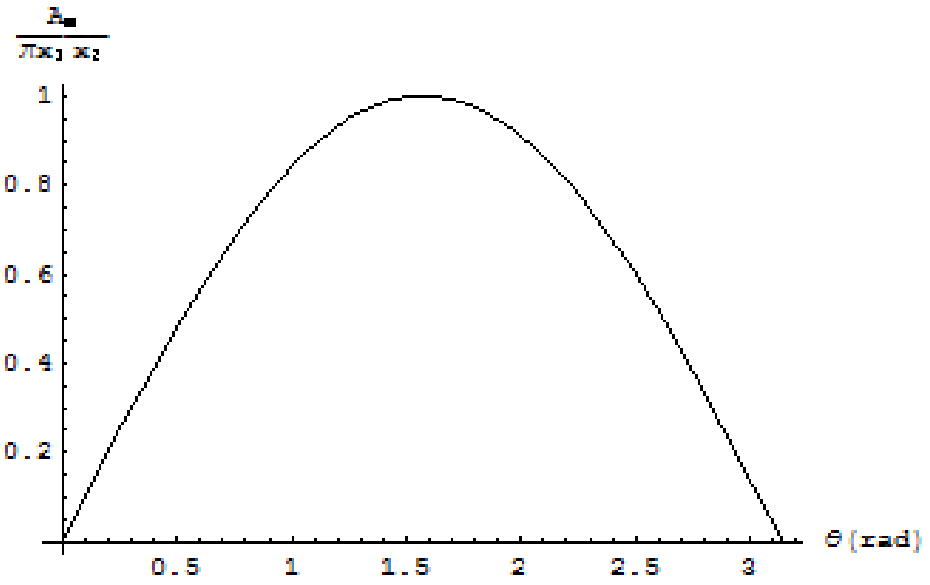

Figure 6.8: Perceived surface area of the metal pipe vs. the angle of incidence

The results of the perceived surface area and angle of incidence are relevant to both the power transmitted to the tag and to the propagation modes as described in Section 6.2.2. These results affect the power transmitted in power density considerations. The density

of power transmitted by a source is related to the area of which the power is dissipated. Typically, the power density allows a calculation of the power transmitted to a single point in space. This is illuminated in Equation 59 below.

$$P_D = \frac{G_R P_{r_T}}{4\pi r^2} \tag{59}$$

The effective power captured by the tag requires consideration of the area of the tag antenna. The effective power received by the tag is portrayed below, where A_{eff} is the effective capture area of the tag antenna.

$$P_{r_{T_t}} = P_{r_T} A_{eff} \tag{60}$$

However, in the case of metal pipes, the perceived area of the metal pipe opening is just as important a consideration. In understanding the phenomena behind angle of incidence, it is obvious that at $\theta \approx 90°$, the perceived surface area of the metal pipe plays a smaller role and therefore the area of the tag antenna is more important. This is so because at those angles the LOS factor plays an important role and the effective tag antenna capture area is smaller in definition with respect to normalization, than the surface area of the metal pipe opening. However, these assumptions are regretfully wrong at the other extremes of angle of incidences. Notice that at $\theta \gg 90°$

and $\theta \ll 90°$, both antenna sizes play a crucial role. Studying these phenomena, it is relieving that a simple equation as depicted below easily solves this problem.

$$A_{eff} = \left[\frac{1}{A_e} + \frac{1}{A_t}\right]^{-1} \tag{61}$$

Using Equation 61 with the general Equation 60, a solution for the system if found, where the perceived area of the metal pipes' opening (A_e) and the area of the tags' antenna (A_t) is taken into consideration. This general solution is shown in Equation 62 below, where $P_{r_{T_t}}$ is the total power received at the tag and P_{r_T} is the power received at the tag before area normalization.

$$P_{r_{T_t}} = P_{r_T}\left[\frac{1}{A_e} + \frac{1}{A_t}\right]^{-1} \tag{62}$$

In the following section, a complete general solution is presented and discussed. It is shown to be a numerical solution that is unique and complete in order to characterize the passive RFID system in metal pipes. This solution is then shown to be a comprehensive theory of passive RFID systems in metal pipes.

6.4 General Theory of Passive RFID Systems in Metal Pipes

The general theory of passive RFID in metal pipes is a theory that incorporates various aspects of the technology and its application to the metal pipe scenario. In this section a general theory is presented that describes the power received by an RFID tag

located in a metal pipe. The tag and therefore the z-axis of the metal pipe need not be within the LOS of the RFID reader system. Since the theory is comprehensive in nature, these irregularities are handled well and the compensation with constant variables are not necessary. The general theory presented in this section is a numerically soluble equation which when subject to the appropriate variable and constant is soluble to a numerical value. Using Equation 62 and Equation 55, the solution is presented in the form depicted in Equation 63 below.

$$P_{r_{T_t}} = 10\log_{10}\left[\left(\frac{\lambda}{4p}\right)^2 G_t G_r \left[P_t - \sum_0^{nl}\left\{P_{loss_{TE_{nl}}} + P_{loss_{TM_{nl}}}\right\}\right] p \frac{1}{r^N} \frac{1}{\left(1+\frac{r}{R_o}\right)^{N_B-2}}\right]\left[\frac{1}{A_e} + \frac{1}{A_t}\right]^{-1} \quad (63)$$

Although this equation is comprehensive, it still lacks the important characteristics of the perceived radius of the metal pipe, especially when considering the transverse modes and the cutoff frequencies. It is well known from the previous sections that the cutoff frequency for the metal pipe is strongly dependent on the radius of the metal pipe. However, in a situation where the angle of incidence is not 90°, the perceived surface area of the metal pipes' opening is dictated by Equation 58. This equation is based on the perceived radius which is exemplified in Equation 57 instead. Using this notion, it is obvious that the general solution needs modification to accept the changes caused by the angle of incidence on the cutoff frequency, propagation modes and therefore internal attenuation. In turn, the changes to the internal attenuation of the

system will relate a direct change to the $P_{loss_{TE_{nl}}}$ and $P_{loss_{TM_{nl}}}$ multi-variable functions as variables to the general solution as noted in Equation 63. Using the information derived from this paper and in Section 6, the comprehensive general theory of passive RFID systems in metal pipes is presented in Equation 64 below along with all the supporting functions and equations.

$$P_{r_{T_t}} = 10\log_{10}\left[\left(\frac{\lambda}{4p}\right)^2 G_t G_r \left[P_t - \sum_0^{nl}\left\{P_{loss_{TE_{nl}}} + P_{loss_{TM_{nl}}}\right\}\right] p \frac{1}{r^N} \frac{1}{\left(1+\frac{r}{R_o}\right)^{N_B-2}}\right]\left[\frac{1}{A_e} + \frac{1}{A_t}\right]^{-1} \quad (64)$$

$$P_{loss_{TM_{nl}}} = \frac{20R_s}{d' a \sin\theta\eta \ln 10}\left[1 - \left(\frac{f_{C_{TM_{nl}}}}{f}\right)^2\right]^{-\frac{1}{2}} \quad (65)$$

$$P_{loss_{TE_{nl}}} = \frac{20R_s}{d' a \sin\theta\eta \ln 10}\left[1 - \left(\frac{f_{C_{TE_{nl}}}}{f}\right)^2\right]^{-\frac{1}{2}}\left[\left(\frac{f_{C_{TE_{nl}}}}{f}\right)^2 + \frac{n^2}{s_{nl}^2 - n^2}\right] \quad (66)$$

$$R_o = \frac{4h_1 h_2}{\lambda} \quad (67)$$

$$A_e = \pi a \sin\theta\, x_1 \quad (68)$$

$$R_s = \frac{1}{\sigma_c f} = \sqrt{\frac{\pi f \mu}{\sigma_c}}, \sigma_c \approx 10^7 \quad (69)$$

$$d' = \frac{d}{\cos\theta} = d\sec\theta \tag{70}$$

$$\eta = \sqrt{\frac{\mu}{\varepsilon}} \tag{71}$$

$$f_{C_{TM_{nl}}} = \frac{t_{nl}}{2\pi a\sqrt{\mu\varepsilon}} \tag{72}$$

$$f_{C_{TE_{nl}}} = \frac{s_{nl}}{2\pi a\sqrt{\mu\varepsilon}} \tag{73}$$

Where 64 is the general theory of the power received at the RFID tag in the metal pipe. Similarly, the power of the received signal at the reader system can be calculated. The equation that dictates the received signal strength of the RFID tag backscatter must encompass the tag backscatter inefficiency as well as the silicon processing power usages. Modeling the entire tag inefficiency as the parameter η_T, the general theory developed above is used to define the received power of the signal at the reader system. The generalized solution is given in Equation 74 below, where $0 \leq \eta_T < 1$. Notice that when $\eta_T = 0$, the tag is not functioning and $\eta_T \neq 1$, since an ideal tag with no power consumption does not exist.

$$P_{r_{R_t}} = 2\frac{P_{r_{T_t}}}{\eta_T} \tag{74}$$

From the general theory in Equation 64, it is easily noticed that no account is made for the propagation below the cutoff frequencies. In order to account for this phenomenon, a new set of equation needs to surface in the general theory. At frequencies below the cutoff, the transverse electric and transverse magnetic modes do not theoretically exists. Therefore, this means that no energy propagates in any wave modes at or above the dominant transverse electric mode. Power from the electromagnetic waves do not propagate through the metal pipe opening and in fact get reflected of the surface plane. This higher level of shielding creates extremely high attenuation constants, which are typically modeled using Equation 75 below, where β' is the measure of phase shift per unit length and is called the phase constant or wave number, and u is the wave velocity.

$$\alpha_{bc} = \beta' \sqrt{\left(\frac{f_c}{f}\right)^2 - 1} \tag{75}$$

$$\beta' = \frac{\omega}{u} = \frac{2\pi f}{u} \tag{76}$$

Substituting Equation 76 into Equation 75, and solving the attenuation function in decibels per meter instead of the units nepers per meter, the following function is derived.

$$\alpha_{bc} = 20 \log_{10} e \frac{2\pi}{c} f \sqrt{\left(\frac{f_c}{f}\right)^2 - 1} \tag{77}$$

To exemplify this equation for a UHF-based passive RFID system, the appropriate values as shown below is inserted into Equation 77 to reveal Equation 78 below.

$$\alpha_{bc} = 20\log_{10} e\frac{2\pi}{c}(915 * 10^6)\sqrt{\left(\frac{f_c}{915*10^6}\right)^2 - 1} = 166.454\sqrt{\left(\frac{f_c}{915*10^6}\right)^2 - 1} \quad (78)$$

Notice that the minimum attenuation as dictated by Equation 78 for a UHF-based passive RFID system is $166.454\ db/m$. Also notice that the attenuation felt during below cutoff is complementary in nature to the attenuation felt by the RFID tag in the metal pipe above cutoff. This is so, such that P_L of Equation 50 and subsequently Equation 64 never exist at the same instance when α_{bc} exists. This is by definition correct and both analytically and theoretically correct as depicted in the equations above. Since the functions behave similar to each other, Equation 53 is very easily modified into the equations below.

$$P_{L_{bc}} = \alpha_{bc} d \quad (79)$$

$$P'_{t_t} = P_t - Re\{P_L\} - Re\{P_{L_{bc}}\} = P_t - Re\{P_L + \alpha_{bc} d\} \quad (80)$$

Finally, substituting Equation 80 back into the general theory, a complete description is now evident with both the sides of the cutoff frequencies considered. This equation is

therefore well suited for any type of analysis within most boundary condition limitations. The modified general theory is presented in Equation 81 below using the set of equations as presented previously (Equations 65 through 73) and Equation 80 above. An expansion of the all incorporated terms is evident in Equation 82 that follows.

$$P_{r_{T_t}} = 10\log_{10}\left[\left(\frac{\lambda}{4p}\right)^2 G_t G_r \left[P_t - Re\left\{\sum_0^{nl}\left\{P_{loss_{TE_{nl}}} + P_{loss_{TM_{nl}}}\right\} + \alpha_{bc}d\right\}\right] p\frac{1}{r^N}\frac{1}{\left(1+\frac{r}{R_o}\right)^{N_B-2}}\right]\left[\frac{1}{A_e}+\frac{1}{A_t}\right]^{-1} \quad (81)$$

$$P_{r_{T_t}} = 10\log_{10}\left[\left(\frac{\lambda}{4p}\right)^2 G_t G_r \left[P_t - Re\left\{\sum_0^{nl}\left\{\frac{20R_s}{d'a\sin\theta\eta\ln 10}\left[1-\left(\frac{f_{C_{TE_{nl}}}}{f}\right)^2\right]^{-\frac{1}{2}}\left[\left(\frac{f_{C_{TE_{nl}}}}{f}\right)^2 + \frac{n^2}{s_{nl}^2-n^2}\right] + \frac{20R_s}{d'a\sin\theta\eta\ln 10}\left[1-\left(\frac{f_{C_{TM_{nl}}}}{f}\right)^2\right]^{-\frac{1}{2}}\right\} + 20\log_{10} e\frac{2\pi}{c}df\sqrt{\left(\frac{f_c}{f}\right)^2-1}\right\}\right] p\frac{1}{r^N}\frac{1}{\left(1+\frac{r}{R_o}\right)^{N_B-2}}\right]\left[\frac{1}{A_e}+\frac{1}{A_t}\right]^{-1} \quad (82)$$

In Equation 74, the power received at the reader is approximated using a linear approach. Although this method is a quick way of analyzing the passive system, care must be taken to encompass the problem appropriately. Different technologies such as

passive UHF RFID systems as compared to SAW-based passive RFID systems would operate rather differently. Therefore, a linear system to describe the tag operation as well as return power would yield inappropriate. In Section 6.5, the UHF RFID tag is analyzed. This analysis includes the propagation of the tags backscatter. Characterizing the tag backscatter allows a highly rigorous theoretical and analytical evaluation of the actual workings of a UHF passive RFID tag in metal pipes.

6.5 Backscatter of UHF Passive RFID Tags

Passive RFID tags operating in the UHF band are rapidly growing into the dominant auto-identification technology. These tags were first used successfully as a friend or foe system during World War II. Most major applications for UHF passive technologies are predominantly in supply chain management where asset track, trace and authentication are often viewed as the Holy Grail. The figure below describes the typical UHF system.

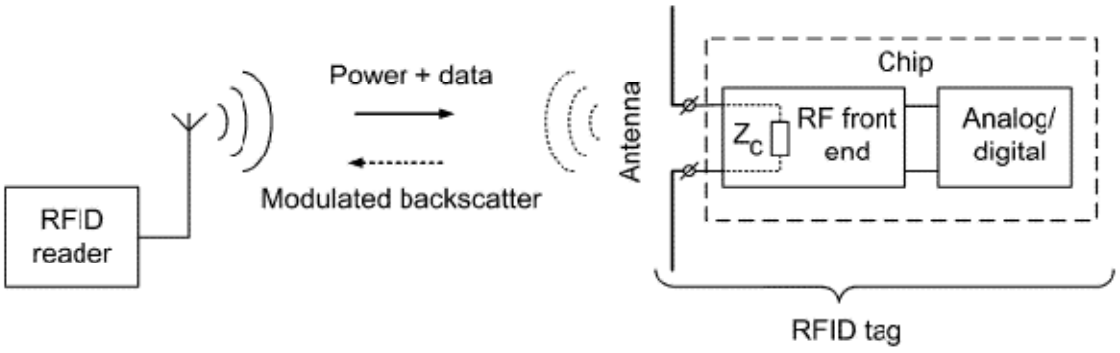

Figure 6.9: Passive UHF RFID System [17]

The purpose of this system is for the reader to identify all the tags in its read zone. This is accomplished by the reader sending a signal aimed directly at tag response. This signal is called the query signal. The passive tag requires energization to power up its application specific integrated circuit (ASIC) and therefore harvests the energy from the RFID readers' carrier wave. Once the tag is able to power up, the reading process starts and the tag moves from the initializing state, up to the identification stage. During the identification stage the tag replies to the reader with a tag ID. Data communication from the tag to the reader is accomplished by switching the tag input impedances' between two states and thus modulating the backscattered signal [18]. This form of data transfer uses various types of modulating schemes [19, 20]. In UHF based passive RFID tags, the application specific integrated circuit is often directly connected to the antenna. The thevenin equivalent of the tag antenna is presented in the figure below.

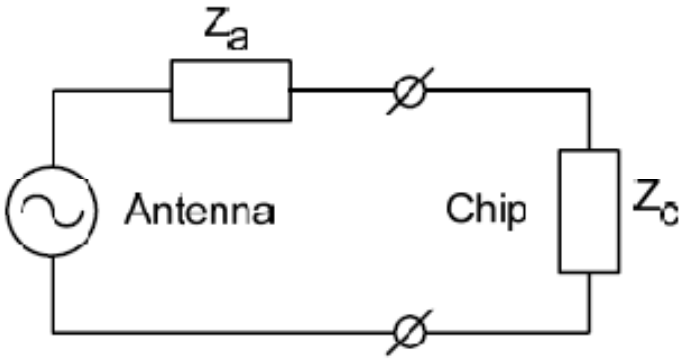

Figure 6.10: Equivalent circuit of an RFID tag [18]

This equivalent circuit above is represented by the impedances Z_a and Z_c as described in Equations 83 and 84 below.

$$Z_a = R_a + jX_a \tag{83}$$

$$Z_c = R_c + jX_c \tag{84}$$

where Z_a and Z_c are the complex antenna impedance and the complex chip (load) impedance respectively. These impedances are typically matched to the high impedance to maximize the collected power [18]. Passive UHF RFID tags typically have positive values for R_a and R_c, negative values for X_c and frequency dependent signs for X_a. The power of the electromagnetic wave in free space is typically modelled well using the modified Friis theory in Equation 42. When considering a tag however, extra care must be taken to include details regarding the effective collection area of the tag antenna and therefore power densities are highly important. Equation 85 below describes the power density of the electromagnetic wave incident on the RFID tag antenna in free space [21].

$$S = \frac{P_t G_t}{4\pi r^2} \tag{85}$$

where P_t is the transmitted power, G_t is the gain of the transmitting antenna and r is the distance between the tag and the reader. To model the power received by the tag

antenna, Equation 85 is multiplied by the effective area of the antenna such as depicted in Equation 86 below. This is the maximum power delivered to the complex conjugated load of Equations 83 and 84.

$$P_a = SA_e \tag{86}$$

where A_e is the effective area of the antenna given by Equation 87 below.

$$A_e = \frac{\lambda^2}{4\pi} G \tag{87}$$

where G is the tag antenna gain. The power of the backscatter signal is the power dissipated by the antenna multiplied by the tag antenna gain [18].

$$P_{re-radiated} = KP_aG \tag{88}$$

where K is the factor that defines the load impedance mismatch. This factor is defined as a contribution of R_a, Z_a and Z_c from Equations 83 and 84 and is calculated using Equation 89. Notice that for real values of antenna impedances a re-radiated power of up to four times more is expected [18]. This assumption fails when the antenna impedance becomes reactive, causing the complex conjugated antenna to re-radiate even more power [17, 18].

$$K = \frac{4R_a^2}{|Z_a + Z_c|^2} \tag{89}$$

Using Equations 83, 84 and 89, Table 6.2 is derived to describe the values for factor K for different values of the antenna load impedances. Similarly, using Table 6.2 and the equations derived above, the backscatter signal strength is deduced and produced in Equation 90.

Table 6.2: Factor K for different antenna load impedances [18]

Z_c	0	Z_a^*	∞
K	$4R_a^2/(R_a^2 + X_a^2)$	1	0

$$P_{re-radiated} = \frac{P_t G_t \lambda^2 R_a^2}{4\pi^2 |Z_a + Z_c|^2 r^2} G^2 \tag{90}$$

Including the inefficiency parameter from Equation 74, a comprehensive description of the tag backscatter is presented and is calculable from Equation 91 below, which is matched parametrically with Equation 82 to reveal Equation 92.

$$P_{backscatter} = \frac{P_t G_t \lambda^2 R_a^2}{4\pi^2 |Z_a + Z_c|^2 r^2} G^2 \eta_T \tag{91}$$

$$P_{r_{R_t}} = \frac{P_{r_{T_t}} G_t \lambda^2 R_a^2}{4\pi^2 |Z_a + Z_c|^2 r^2} G_r^2 \eta_T \tag{92}$$

$$P_{r_{R_t}} = \frac{G_t \lambda^2 R_a^2}{4\pi^2 |Z_a + Z_c|^2 r^2} G_r^2 \eta_T 10 \log_{10} \left[\left(\frac{\lambda}{4p} \right)^2 G_t G_r \left[P_t - Re \left\{ \sum_0^{nl} \left\{ \frac{20R_s}{d' a \sin\theta \eta \ln 10} \left[1 - \left(\frac{f c_{TE_{nl}}}{f} \right)^2 \right]^{-\frac{1}{2}} \left[\left(\frac{f c_{TE_{nl}}}{f} \right)^2 + \frac{n^2}{s_{nl}^2 - n^2} \right] + \frac{20R_s}{d' a \sin\theta \eta \ln 10} \left[1 - \left(\frac{f c_{TM_{nl}}}{f} \right)^2 \right]^{-\frac{1}{2}} \right\} + 20 \log_{10} e \frac{2\pi}{c} df \sqrt{\left(\frac{f_c}{f} \right)^2 - 1} \right\} \right] p \frac{1}{r^N} \frac{1}{\left(1 + \frac{r}{R_o} \right)^{N_B - 2}} \left[\frac{1}{A_e} + \frac{1}{A_t} \right]^{-1} \quad (93)$$

Finally, combining the general theory of the power received at the RFID tag in metal pipes with Equation 92, a comprehensive theory that describes the power of the tag reply signal at the reader is attained. This theory can be calculated from Equation 93 using the supporting functions and Equations (Equations 65 through 73). Section 6.6 describes the readability of the typical passive UHF RFID tag in metal pipes. This section models the readability ratio as a constant ratio of the power transmitted as compared to the received tag reply signal strength. This method provides a complete theoretical evaluation of passive UHF RFID system in metal pipes.

6.6 Readability of UHF Passive RFID Tags

The readability of a tag is a ratio that describes the number of read attempts as compared to the number of actual reads. There are various factors that are typically considered for a readability measurement. Some factors such as range, power, tag and reader antenna designs, application specific integrated circuit design, environments and number of tags in the environments are highly critical to the this ratio. The general theory leading up to the received signal strength (RSS) calculator at the reader as described in Equation 93 considers most of these factors. This theory however does not

consider many other environmental impacts and currently doesn't consider operation of multiple tags, whether it be inside or outside the metal pipes. These environments require advanced theories that would take much more mathematical analysis and computation, and could potentially yield highly unstable sets of equations. However, using the comprehensive theories underlined in this paper, a simplistic description of the readability ratio can be attempted. For the purpose of this paper, assume the definition of read ratio is dependent on the power of the signal transmitted by the reader to the power of the tag reply signal. Then it follows that the readability ratio is calculable using Equation 94 below.

$$R = |\eta_R| \frac{P_{r_{R_t}}}{P_t} = |\eta_R| \frac{P_{r_{R_t}}}{P_{t_{R_t}}} \tag{94}$$

where η_R is the complex readability constant that defines the amplification and noise filtering system in the passive UHF RFID reader and is defined by Equation 95.

$$\eta_R = \eta_a + j\eta_n \tag{95}$$

where η_a is the amplification constant and η_n is the noise filtering constant. The absolute value of the readability constant is calculable using the equation presented below.

$$|\eta_R| = \sqrt{\eta_a^2 + \eta_n^2} \tag{96}$$

The complex readability constant is typically a dynamically changing variable based on events and environments, impacted by time-space and is non-classified as of present. The readability ratio (R) is required to be a real number between 0 and 1 ($0 \leq R \leq 1$). Therefore, the upper and lower bounds of the absolute value of the complex readability constant are defined by the statement presented below.

$$0 \leq |\eta_R| \leq \frac{P_{t_{R_t}}}{P_{r_{R_t}}} \tag{97}$$

In the following section, a qualitative analysis is conducted to analyze and collect information regarding actual tag behavior in different sizes of metal pipes. The metal pipes are chosen to be above and below the cutoff frequency for passive UHF RFID systems. This is used to simulate the passive UHF RFID system at 902MHz to 928MHz. In this exercise, the intent is to collect tag behavior which can then be used to validate the general theory derived in Section 6. While the proceeding section concentrates in accumulating tag related performance in metal pipes, Section 8 will be dedicated to analyzing a sample data set from Section 7 to validate the general theory.

CHAPTER 7

QUALITATIVE ANALYSIS

This section focuses on the experimental test setup and the analytical and qualitative analysis of different UHF tag antenna designs in metal pipes. The tag design used extensively during this process is the quarter wave monopole antenna. The monopole antenna behaves exactly similar to the dipole antenna. It is designed by replacing one half of the dipole antenna with a ground plane at right angles (90°) to the remaining half. This design is chosen because its radiation and gain pattern resembles the majority of passive UHF RFID tags that exist in the market today. The setup for the analytical analysis is broken down into two distinct parts. These parts are the monopole in the z-axis and in the x-axis as depicted in Figures 7.1 and 7.2 below respectively. This analytical analysis is conducted in an electromagnetic environment called Feko 5.3 which is developed using leading computational electromagnetic (CEM) methods. The method used here was the hybrid MoM/FEM which involves the full coupling of metallic environments using MoM methods with the heterogeneous dielectric bodies in the FEM regions. This method is highly accurate for the structure sizes used in this paper. In the following section, the experimental test setup is detailed.

7.1 Experimental Test Setup

The experimentation setup is depicted for both scenarios in the figures below. In Figure 7.1 below, the purple base serves as the ground plane for the monopole antenna in the +z-axis. Notice that in Figure 7.2, the ground plane is the metal pipe itself and the antenna is in the +x-axis which is radial in nature when considering the metal pipe structure. The length of the monopole antenna is a quarter wavelengths in both figures and the metal pipe is designated to 1m in length. The radius of the metal pipe is varied such that it is below and then above cutoff frequencies for all measurements in all axes. In Section 7.2, the results of the analytical analysis are presented.

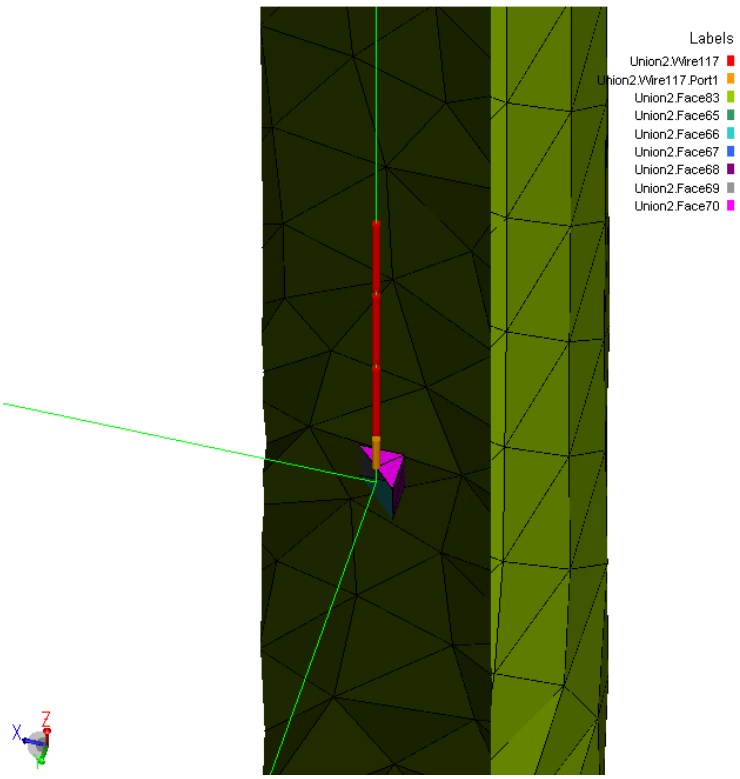

Figure 7.1: Monopole in the +Z Axis

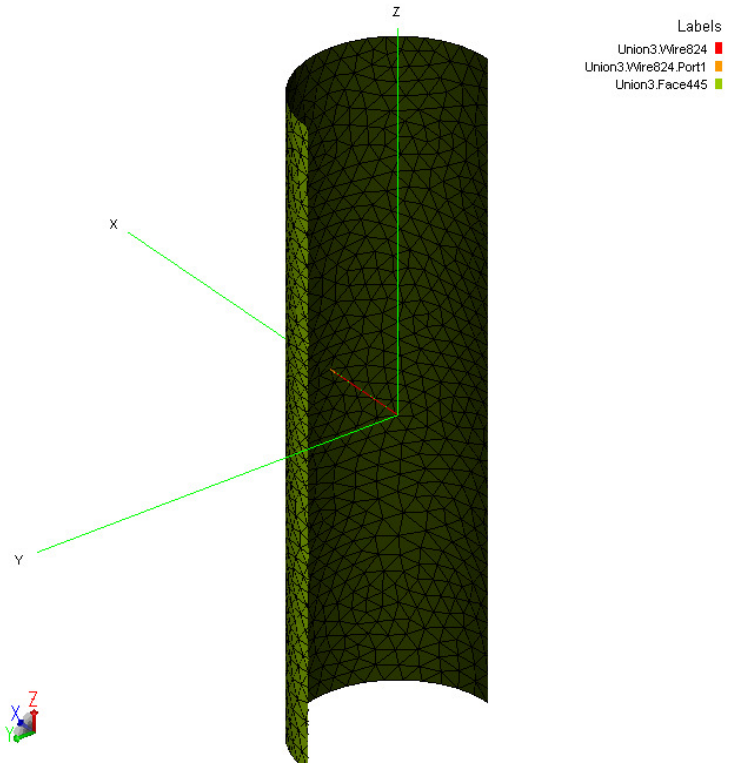

Figure 7.2: Monopole in the +X Axis

7.2 Results

In this section, the results of the analytical analysis is presented for both cases as depicted in Figure 7.3 and 7.4, where the monopole is oriented in the +x-axis and +z-axis respectively. Notice that the maximum gain of the monopole antenna is 1.56 (linear gain) at right angles (90°) to the axis of perspective. This linear gain corresponds to $20\log_{10}(1.56) = 3.86249dB$. In the following sections, the results for the evaluation in the +z-axis and +x-axis is presented for both above and then below the cutoff frequency.

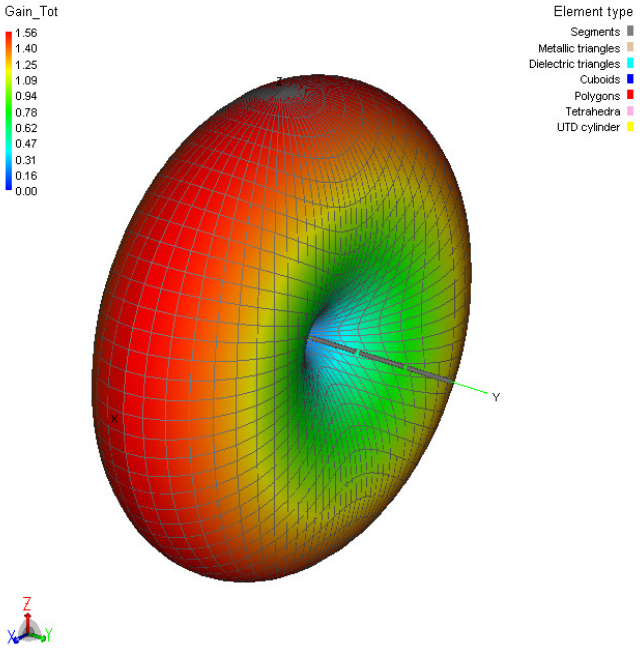

Figure 7.3: Gain pattern for a monopole in the +X Axis

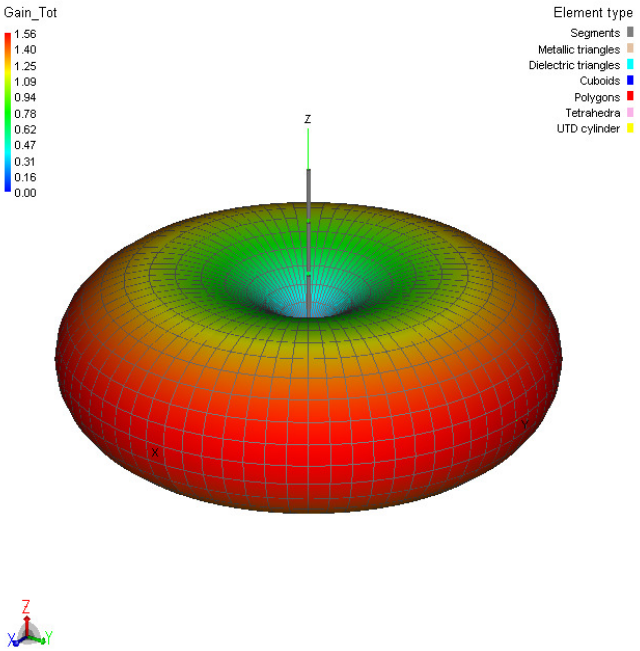

Figure 7.4: Gain pattern for a monopole in the +Z Axis

7.2.1 Quarter-wave Monopole in the +Z Axis

The monopole antenna placed in the +z-axis is located in the centre of the metal pipe. Since the antenna is along the +z axis, the antenna is located from the $L_1 = \{x_1, y_1, z_1\} = \{0,0,0\}$ to the coordinates $L_2 = \{0,0, \lambda/4\}$. As depicted in the figures, the metal pipe is located along the z-axis, where $\{l_{Min}, l_{Max}\} = \{-0.5,0.5\}$. In this setup, L_n is the location of coordinate n, l_{Min} is the starting point for the length of the metal pipe in the +z-axis, l_{Max} is the stopping point for the length of the metal pipe in the +z-axis and all units are in m. The following section will illuminate the results for the setup described above.

7.2.1.1 Above Cutoff Frequency

The results for the tag at the centre of the metal pipe are presented in Figure 7.5 below. Notice that the gain pattern of the tag antenna is allowed to permeate through the metal pipe to enable better visualization. The maximum gain recorded is 2.40 in the –z direction. Notice that at different angles of wave incidence, the gain could vary from 2.40 to 0. This means that if the ray tracing method were used to discover the readability, it would yield highly sensitive to minor changes in the path or angle of incidence. On the other hand, an electromagnetic wave travelling in the path parallel to the z-axis would typically have a gain of 0 and therefore would yield no reads. These results predict that if the reader was pointing directly at the tag from the z-axis, the tag would almost definitely not be read. However, since the reader is not a LOS reader, the reflections of non-parallel rays would increase the probability of reads.

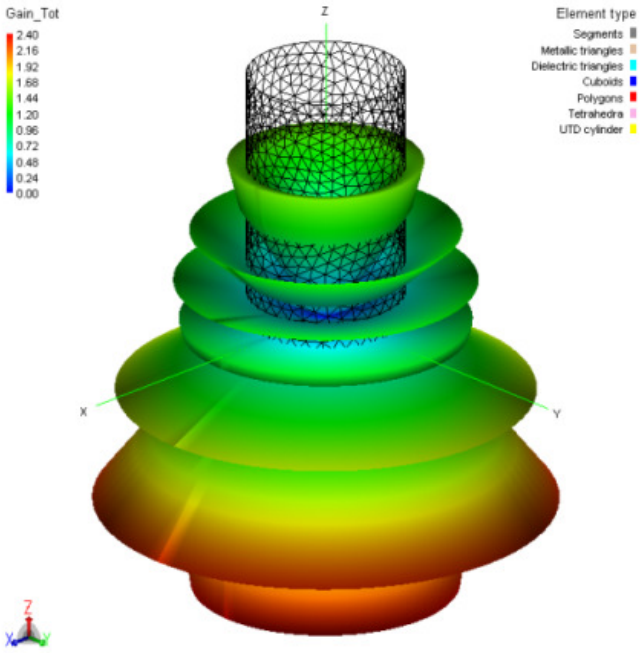

Figure 7.5: Gain pattern of a monopole in the +Z axis at the centre of the metal pipe above cutoff frequency

7.2.1.2 Below Cutoff Frequency

At below the cutoff frequency, notice that for the same tag antenna setup, the maximum linear gain is negative. This is because the power loss using the MoM method is larger than the active power. This typically occurs when the imaginary part of the impedance is large, thus causing the real part to be highly inaccurate. This means that under most conditions, the tag would not be read at the centre of a meter long metal pipe. In Section 7.2.2, the quarter-wave monopole is investigated for the case when it is aligned radially along the +x-axis of the metal pipe.

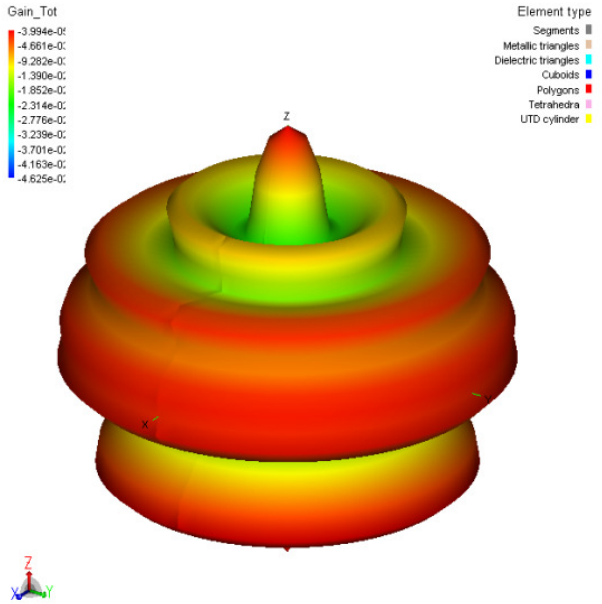

Figure 7.6: Gain pattern of a monopole in the +Z axis at the centre of the metal pipe below cutoff frequency

7.2.2 Quarter-wave Monopole in the +X Axis

The quarter-wave monopole is aligned in the +x-axis and analyzed for both above and below cutoff frequency. The tag is positioned such that the antenna is located from the $L_1 = \{x_1, y_1, z_1\} = \{-r, 0,0\}$ to the coordinates $L_2 = \{\lambda/4 - r, 0,0\}$, where r is the radius of the metal pipe. As depicted in Figure 7.7, the metal pipe is located along the z-axis, where $\{l_{Min}, l_{Max}\} = \{-0.5,0.5\}$.

7.2.2.1 Above Cutoff Frequency

Notice that when subject to a region above cutoff, the monopole behaves differently when compared with Figure 7.5. This shows that the direction of the antenna is absolutely critical. From Figure 7.7 below, if the reader is LOS and parallel to the z-axis, the probability of reads are extremely high. However, non-LOS rays could

potentially not be read since the tag antenna gains are lower for any angles beside LOS. Therefore, the monopole antenna in the +x-axis works well when the reader and tag are aligned but do not work as well when non-LOS ray tracing is required. Comparing Figure 7.5 and Figure 7.7, it is obvious that there exist differing gain patterns for the tag antenna when directionality of the tag antenna changes.

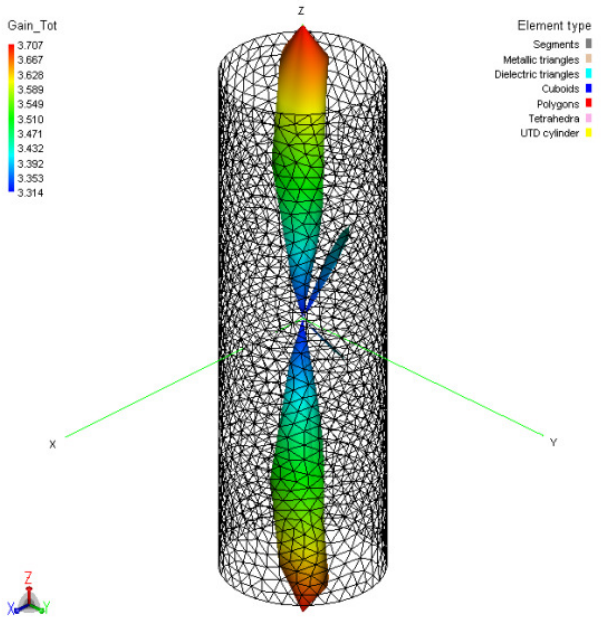

Figure 7.7: Gain pattern of a monopole in the +X axis at the centre of the metal pipe above cutoff frequency

7.2.2.2 Below Cutoff Frequency

Analyzing the results for the monopole in the +x-axis under below cutoff conditions, it is recognized that the gain patterns do not reflect negative values as for the case depicted in Figure 7.6. However, the results as presented in Figure 7.8 show that the gain of the tag antenna are two orders of magnitude lower than the maximum tag

antenna gain in free space. Furthermore, the maximum gain is in the x-axis direction which is perpendicular to the surface of the metal pipe and therefore would not allow any successful reads. A brief conclusion from analyzing tag antennas working below cutoff is that they would not yield any reads in most conditions. However, for cases when the tags are extremely close to the mouth of the metal pipe, high attenuations could still allow some tags to be read. Nevertheless, these reads are typically insignificant and would be highly dependent on the LOS of the reader antenna as well as the direction of the tag antenna.

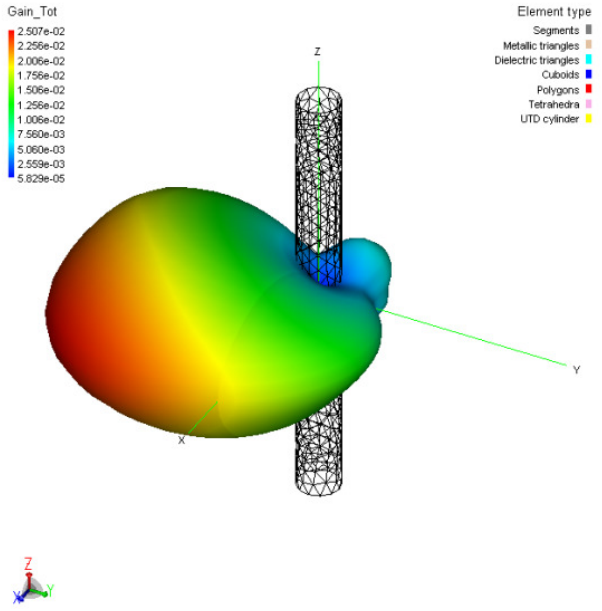

Figure 7.8: Gain pattern of a monopole in the +X axis at the centre of the metal pipe below cutoff frequency

In the following section, further results are presented for special antenna designs. The designs considered here are the helical antenna in the +z-axis and the cone shaped helical antenna in the +z-axis.

7.3 Further Results

Helical antenna designs consist of a conducting wire wound to form a helix. The parameters that dictate the way helical antenna's operate include the number of turns, direction of the turns, spacing between the turns, the circumference of the helix, the impedances and the wavelength of the electromagnetic waves. The directive gain of the helical antenna in free space is modeled well by the equation presented below.

$$D_o \cong 15N\frac{C^2S}{\lambda^3} \tag{98}$$

where N is the number of turns, C is the circumference, S is the spacing between each turn and λ is the wavelength. In the case of a cone shaped helical antenna, the value of the directive gain is dynamic and therefore a complex directive gain is accumulated in Equation 98. This function can therefore be substituted directly into Equation 93 for the purpose of the analysis. In the proceeding sections, the results of the analytical evaluations for both types of helical antennas are presented.

7.3.1 Helical Antenna in the +Z Axis

Figure 7.9 illustrates the gain pattern for the helical antenna in the +z-axis. The purpose of this illustration is to present the typical directive gain plot for an antenna structure of such. Notice that the directive gain is higher in magnitude in the reverse –z

direction. The helical antenna in this figure is designed using left handed wounding and has the diameter of $\lambda/4$ and $N = 10$. The right hand wounding would produce a similar gain pattern with the higher magnitude side on the +z direction instead.

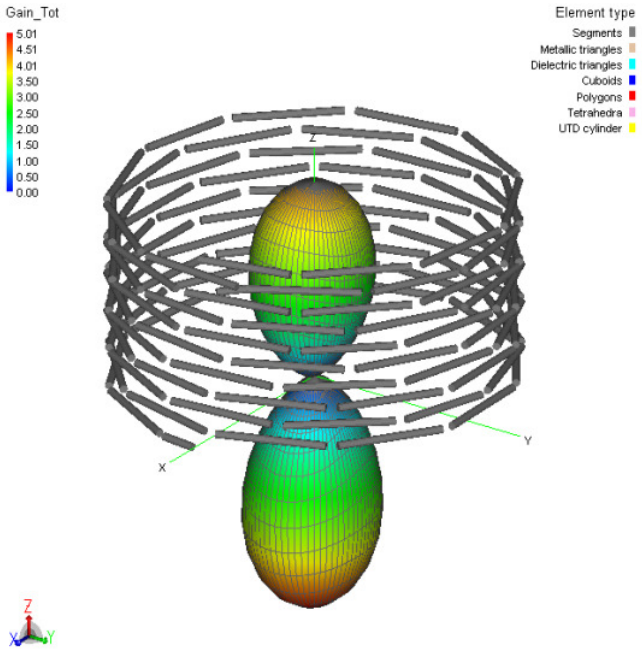

Figure 7.9: Gain pattern of a helical antenna in the +Z axis

The effective gain patterns inside a metal pipe above cutoff frequency for the helical antenna in Figure 7.9 is presented in Figure 7.10 below. The helical antenna is placed at the origin and centre of the metal pipe, while the metal pipe is located along the z-axis, where $\{l_{Min}, l_{Max}\} = \{-0.25,0.75\}$.

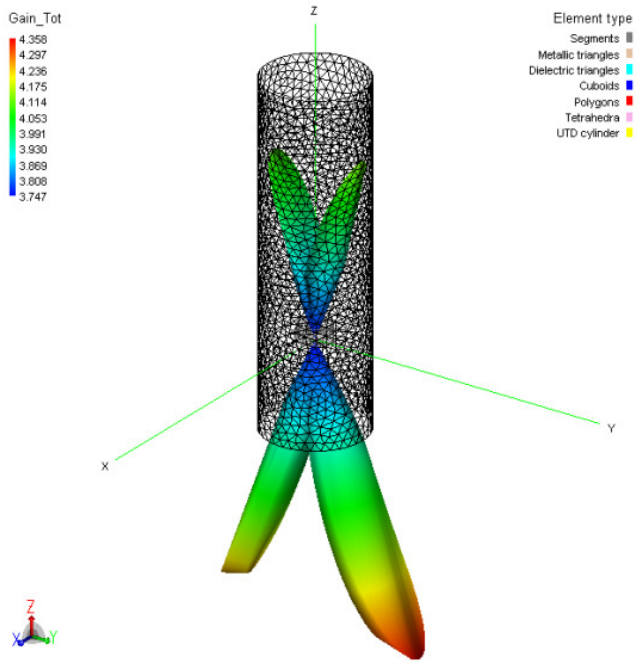

Figure 7.10: Gain pattern of a helical antenna in the +Z axis at the centre of the metal pipe above cutoff frequency

Notice that the gain patterns observed from the helical antenna is awkwardly positioned at various angles. This type of gain patterns typically allow the passive tag to increase its performance but still lacks the robustness required in a metal pipe environment. The purpose of the helical antenna design is to enable a high spread gain throughout the metal pipe. Although the results from helical design seems to give higher magnitudes of directional gain, the non-comprehensive coverage area of the gain patterns are not up to standards with the requirements of tagging in metal pipes. The final design studied in this paper is the cone shaped helical antenna presented in the following section.

7.3.2 Cone Shaped Helical Antenna in the +Z Axis

The cone shaped antenna design typically allows a more dynamic nature for the gain patterns. This is reflected by the 2-dimensional intersection caused by the conical structure. The angle of intersection is modified for a high gain while maintaining directionality. The results for the gain of a cone shaped helical antenna are presented in Figure 7.11 below. Notice that the directional gain of the cone shaped helical antenna can be approximated using the dynamically modified version of Equation 98. Another method to analyze this design is by using the methods used to approximate helical antennae with cylindrical cups as the bases. When using this method, care must be taken to reflect the image of the directional gains.

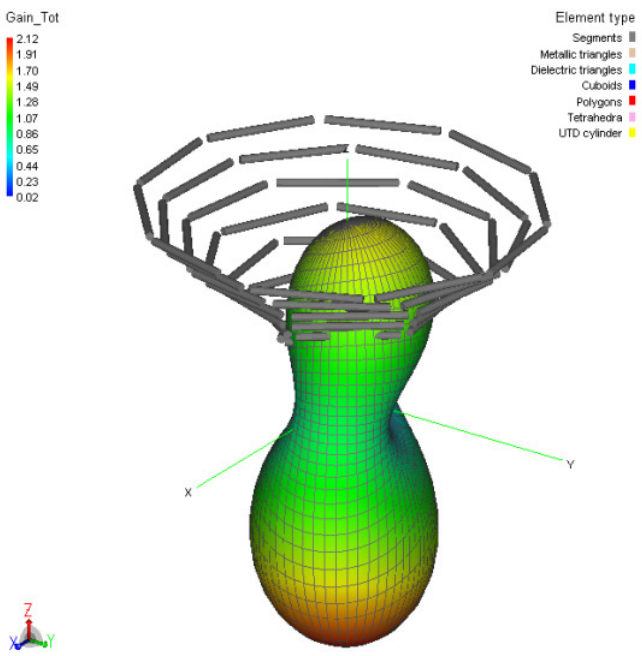

Figure 7.11: Gain pattern of a cone shaped helical antenna in the +Z axis

Figure 7.12 represents the cone shaped helical antenna design in the metal pipe. The helical antenna is placed at the origin and centre of the metal pipe, while the metal pipe is located along the z-axis, where $\{l_{Min}, l_{Max}\} = \{-0.25, 0.75\}$. Notice that the metal pipe actually works as an amplification process for the gain of this type of helical antenna. This is caused by the wounding of the antenna and by the 2-dimensional conical line intersections as discussed earlier. Also, notice that the gain pattern of this type of antenna seems to satisfy to some extent the requirements for the comprehensive coverage area.

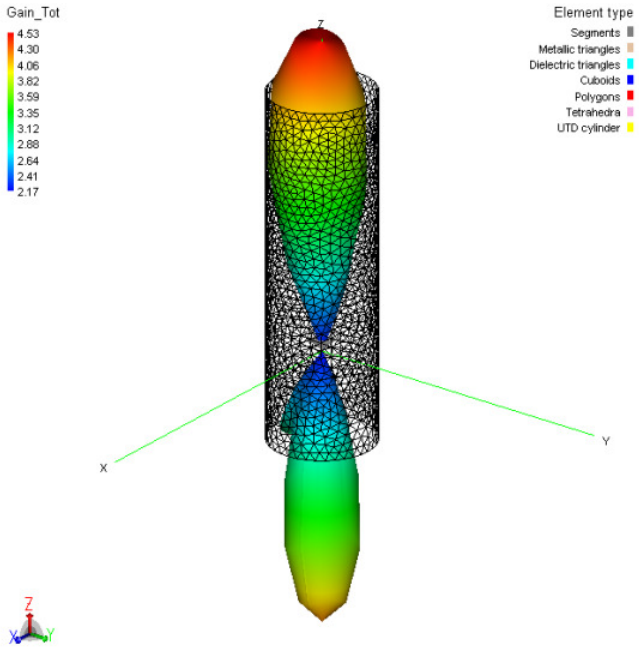

Figure 7.12: Gain pattern of a cone shaped helical antenna in the +Z axis at the centre of the metal pipe above cutoff frequency

Using a design similar to this would therefore allow the successful tagging of metal pipes when used in conjunction with the general theory of RF propagation as derived in Equation 93. In the following section, discussions regarding the analytical evaluations in presented. This section also describes the theoretical evaluations found in Section 6.

CHAPTER 8

DISCUSSION

In this section, the body of work proposed and evaluated is used to predict the workings of a passive UHF RFID tag with a cone shaped helical antenna. The details of the design include the complex conjugate impedances in the application specific integrated circuit and the assumptions generalized in Section 6. From Figure 7.12 in Section 7, the gain pattern of a cone shaped helical antenna is depicted in Figure 8.1 below and can be represented by Equations 99 and 100.

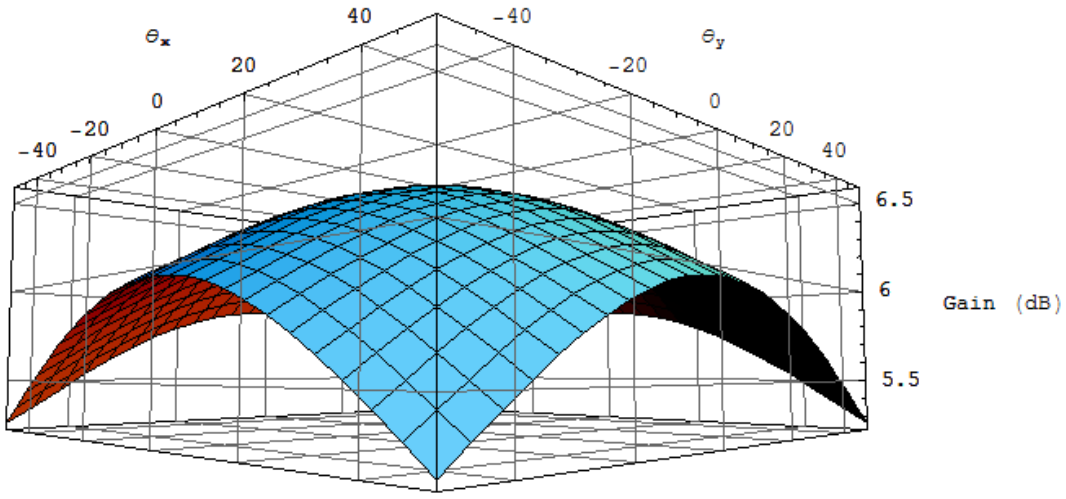

Figure 8.1: Gain of the cone shaped helical antenna (dB) vs. angle from z-axis

$$G_T = G_{T_t} - \theta^2 \tag{99}$$

$$G_T(dB) = 10\log_{10}\left[G_{T_t} - \theta^2\right] \tag{100}$$

This function is a generalized description of the cone shaped helical tag antenna, and when inserted in Equation 93, calculates the received signal strength in dBm at the reader. The environment conditions and constant variables are as described above, similar to the assumptions made in Section 6.

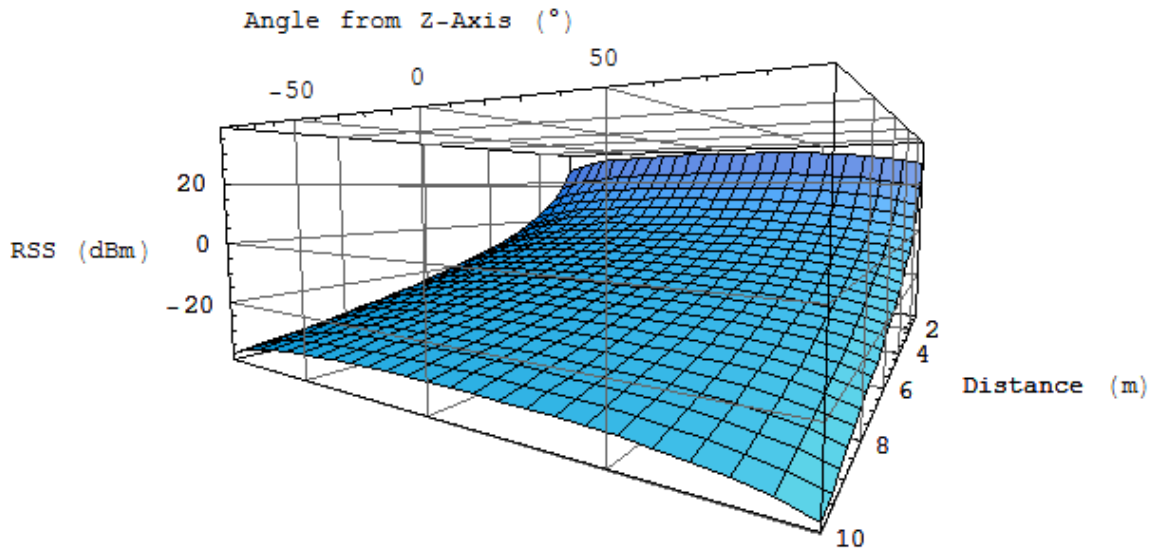

Figure 8.2: Received signal strength at the tag vs. distance and angle from the z-axis for the cone shaped helical antenna

Figure 8.2 depicts the received signal strength in dBm when calculated using the equations developed in Section 6 for the power at the tag. This plot is generated for the variable distance between the reader and the surface of the metal pipe. Notice that the effects of the angle of incidence tend to reduce the signal strength slightly but is typically linear in nature. This requires a complex explanation that involves both

deterministic and idealistic constructive as well as destructive interferences and will be tackled in further publications. An easy way to explain this is that ray's incident on the surface of the metal pipe at higher angles, typically have a longer path to the source and therefore tend to lose more power due to propagation. Although this simplistic assumption is true, the actual reasons for this effect are highly mathematically involving.

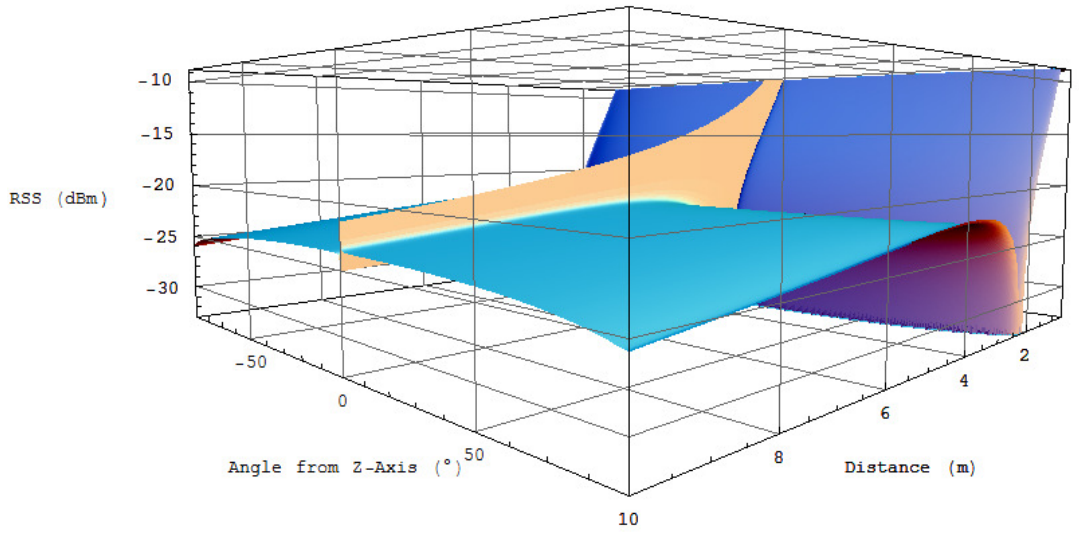

Figure 8.3: Received signal strength at the reader vs. distance and angle from z-axis in an over sampled environment from the [1, 1, 1/2] viewpoint

Figure 8.3 depicts the received signal strength at the reader system for given distance between the reader and the surface opening of the metal pipe, as well as the angle from the z-axis. Notice that the variations are manifolds and not directly predictable using judgment and intuition. Notice that the uncertainty in the centre of the metal pipe could yield an averaged readability ratio of up to 0.5 if the nominal read ratio is for the

received signal strength of approximately -23dBm, when analyzed using the theory developed in Section 6. Also notice that there are interesting occurrences closer to the boundary conditions of the metal pipe and free propagation space. In the proceeding section, a comprehensive conclusion is presented that summarizes the workings of passive RFID tags in metal pipes.

CHAPTER 9

CONCLUSION

In this paper, the characteristics of RF propagation in metal pipes are studied for passive RFID systems. It is found that there are various variables that contribute to the performance and readability of passive UHF tags in metal pipes. Using the theory developed in this paper, parameters for specific passive RFID systems are chosen and analyzed. These theoretical and analytical evaluations show that the performance of passive RFID tags in metal pipes are complex in nature. These complexities are further discussed to reveal the nature of the received signal strength of the passive reader system for tags in a given metal pipe. The general theory presented in this paper allows the straight forward evaluation of passive RFID systems when used intrinsically or extrinsically in metal pipes. This theory is also derived to include fundamental constraints of the operating environment. Finally, analytical results and compelling discussions are presented for the workings of passive RFID systems in metal pipes.

The far field gain patterns presented in this paper are indeed a good justification of the need for a theory to comprehend the workings of passive RFID tags in metal pipes. It is shown that the operation of a tag is very different below cutoff frequencies than they are above cutoff frequencies in metal pipes. Another interesting area of study would be the characterization of passive RFID tags and systems in rectangular metal pipes. Although some work previously have enlightened us on the detail workings of

RF devices or communication in metallic environments [22-52], these works have only concentrated on cylindrical tunnels. As pointed in Section 5, cylindrical metal pipes are modeled using the unique Bessel function which models the propagation well in a circular waveguide. Although its rectangular counterpart has been studied thoroughly, there still does not exist any work analyzing the currently existing knowledge on these rectangular EM structures with passive RFID technology. As pointed out earlier on, passive UHF RFID tags are very susceptible to the environment that they operate in. Because of its nature of harvesting energy for the powering of the ASIC and because of the backscatter communications, the passive tag is very sensitive to metallic environments. This causes the passive tag to operate different around metallic objects such as the metal pipe.

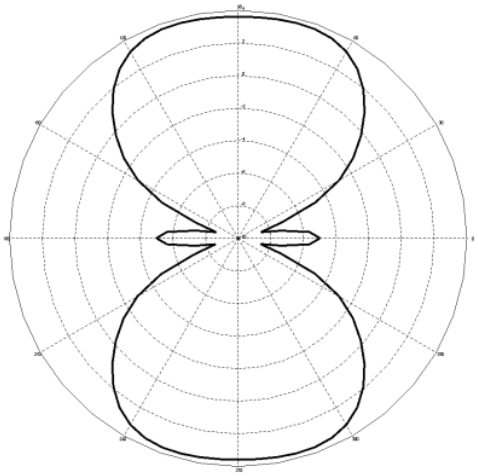

Figure 9.1: 2D polar plot of the far field gain pattern for the loaded meander tag antenna in a rectangular metal pipe above cutoff frequencies

Figure 9.1 is a polar plot of the far field pattern for a loaded meander tag antenna in a rectangular metal pipe above cutoff frequencies. We can see that this information used along with the theory presented in the previous sections would allow us to quantify the workings of any specific RFID tag operating within metal pipes. Interestingly, during above cutoff, the gain of the tag antenna is almost always almost doubled which will allow us to substantiate that the theory would yield high read rates at above cutoff. Nevertheless, the proposed theory would still allow us to determine the actual performance of the tag based on many other factors such as angle of incidence of the planar waves as well as effective area and actual cutoff relationships. When operated below cutoff, the theory will allow for guided usage, as it will allow calculations of the tags workings. Since there is potential for a tag to work even below cutoff frequencies, it is obvious that this operations could be fully understood using the theory derived for cylindrical metal pipes in this paper. The common areas for improvement are the fact that this theory still has no proper ability to comprehend the tag antenna gains itself, and therefore will required gain plots such as in Figure 9.1 before it can be used substantially and successfully. This is an inherent problem that will be dwelled on for further publications. In developing the theory, it was realized that these theories can potentially be merged for a unification of any metallic objects that appear as cutoff mechanisms. This is something that will be tackled in further publications. Finally, it is shown that there exists more room for improvements within the theory itself, as it still lacks comprehensiveness. These comprehensive needs such as the proposed theoretical gain predictions are difficult in a broader scope, but attainable when focused to just

metallic objects that appear to have cutoff mechanisms. In further publications, we will explore these methods and mechanisms in an attempt to broaden our knowledge on the workings of passive UHF RFID systems near or around metallic enclosures with cutoff mechanisms.

REFERENCES

[1] Finkenzeller, K., Fundamentals and Applications in Contactless Smart Cards and Identification, John Wiley & Sons, LTD, ISBN 0-470-84402-7, 2003.

[2] IDTechEx Ltd.

[3] Robertson, I.D., Jaialy, I., "RF id tagging explained", Communications Engineer, Vol 1, pp 20-23, 2003.

[4] Engels, W. Daniel, "Review of RFID Technologies", UTA TxRF Memo, UTA, TxRF-001, January 2007.

[5] Kim, K.Y., Tae, H-K. and Lee, J-H. (2003) 'Analysis of leaky modes in circular dielectric rod waveguides', *Electronic Letters*, Vol. 39, No. 1, pp.61–62.

[6] Sadiku, M.N.O. (1989) *Elements of Electromagnetism*, Saunders College Publishing, LTD, ISBN 0-03-094947-5.

[7] Cheng, D.K. (1993) *Fundamentals of Engineering Electromagnetics*, Addison-Wesley Publishing Company, LTD, ISBN 0-201-56611-7.

[8] Dudley, D.G., Lienard, M., Mahmoud, S.F. and Degauque, P. (2007) 'Wireless propagation in tunnels', *IEEE Trans. on Antennas and Propagation*, Vol. 49, No. 2, pp.11–26.

[9] Dudley, D.G. (2005) 'Wireless propagation in circular tunnels', *IEEE Trans. on Antennas and Propagation*, Vol. 53, No. 1, pp.435–441.

[10] Dudley, D.G. and Mahmoud, S.F. (2006) 'Linear source in a circular tunnel', *IEEE Antennas and Propagation*, Vol. 54, No. 7, pp.2034–2047.

[11] Perera, S.C.M., Williamson, A.G. and Rowe, G.B. (1999) 'Prediction of breakpoint distance in microcellular environments', *Electronic Letters*, Vol. 35, No. 14, pp.1135–1136.

[12] Arumugam, D.D., 'The Basics of RFID Systems', UTA TxRF Memo, UTA, TxRF-003, January 2007.

[13] Rustako Jr., A.J., Amitay, N., Owens, G.J. and Roman, R.S. (1991) 'Radio propagation at microwave frequencies for line-of-sight microcellular mobile and

personal communications', *IEEE Transactions on Vehicle Technology*, Vol. 40, No. 1, pp.203–210.

[14] Sarkar, T.P., Ji, Z., Kim, K., Medouri, A. and Salazar-Palma, M. (2003) 'A survey of various propagation models for mobile communications', *IEEE Antennas and Propagation* Magazine, Vol. 45, No. 3, pp.51–82.

[15] Tan, S.Y. and Tan, H.S. (1995) 'Improved three dimensional ray tracing technique for microcellular propagation models', *Electronic Letters*, Vol. 31, No. 17, pp.1503–1505.

[16] Arumugam, D.D., Engels, D.W. and Modi, A. (2007) 'Environmental and performance analysis of SAW-based RFID systems', *Int. J. Radio Frequency Identification Technology and Applications*, Vol. 1, No. 2, pp.203–235.

[17] Rao, K.V.S., Nikitin, P.V. and Lam, S.F. (2005) 'Antenna design for UHF RFID tags: A review and a practical application', *IEEE Trans. on Antennas and Propagation*, Vol. 53, No. 12, pp.3870–3876.

[18] Nikitin, P.V. and Rao, K.V.S. (2006) 'Theory and measurement of backscattering from RFID tags', *IEEE Trans. on Antennas and Propagation*, Vol. 48, No. 6, pp.212–218.

[19] Glidden, R. (2004) 'Design of ultra-low-cost UHF RFID tags for supply chain applications', *IEEE Communication Magazine*, Vol. 42, No. 8, pp.140–151.

[20] Curty, J.-P., Joehl, N., Dehollain, C. and Declercq, M.J. (2005) 'Remotely powered addressable UHF RFID integrated system', *IEEE Journal of Solid-State Circuits*, Vol. 40, No. 11, pp.2193–2202.

[21] Nikitin, P.V., Rao, K.V.S. and Martinez, R.D. (2007) 'Differential RCS of RFID tag', *Electronics Letters*, Vol. 43, No. 8, pp.431–432.

[22] Elliot, R.S. (2003) *Antenna Theory and Design*, IEEE Press Series on Electromagnetic Wave Theory, Wiley-Interscience, ISBN 0-471-44996-2.

[23] J. I. Glaser, "Low Loss Waves in Hollow Dielectric Tubes," PhD Thesis, MIT, February 1967.

[24] J. I. Glaser, "Attenuation and Guidance of Modes in Hollow Dielectric Waveguides," *IEEE Transactions on Microwave Theory and Techniques*, MTT-17, March 1969, pp. 173-174.

[25] S. F. Mahmoud, *Electromagnetic Waveguides: Theory and Applications*, Stevenage, England, Peter Peregrinus, 1991.

[26] K. D. Laakmann and W. H. Steier, "Waveguides: Characteristic Modes of Hollow Rectangular Dielectric Waveguides," *Applied Optics*, 15, 1976, pp. 1334-1340.

[27] J. M. Molina-Garcia-Pardo, M. Lienard, P. Degauque, D. G. Dudley and L. Juan-Llacer, "MIMO Channel Characteristics in Rectangular Tunnels from Modal Theory," *IEEE Transactions on Vehicular Technology*, in review, 2006.

[28] S. F. Mahmoud and J. R. Wait, "Guided Electromagnetic Waves in a Curved Rectangular Mine Tunnel," *Radio Science*, 9, 1974, pp. 567-572.

[29] Dudley, D. G. and Pao, H.-Y., 'System Identification for Wireless Propagation Channels in Tunnels ', *IEEE Transactions on Antennas and Propagation*, AP-53, No. 8, 2005, pp.2400–2405.

[30] Holloway, C.L., Hill, D.A., Dalke, R.A., and Hufford, G.A., 'Radio Wave Propagation Characteristics in Lossy Circular Waveguides Such as Tunnels, Mine Shafts, and Boreholes', *IEEE Transactions on Antennas and Propagation*, AP-48, No. 9, 2000, pp.1354–1365.

[31] Ruskeepaa, H., *Mathematica Navigator*, Amsterdam, Elseveir, 2004.

[32] Mahmoud, S. F. and Wait, J.R., 'Geometrical Optical Approach for Electromagnetic Wave Propagation in Rectangular Mine Tunnels', *Radio Science*, No. 9, 1974, pp.1147–1158.

[33] Mariage, P., Lienard, M., and Degauque, P., 'Theoritical and Experimental Approach of the Propagation of High Frequency Waves in Road Tunnels', *IEEE Transactions on Antennas and Propagation*, AP-42, No. 1, 1994, pp.75–81.

[34] Lienard, M. and Degauque, P., 'Natural Wave Propagation in Mine Environments', *IEEE Transactions on Antennas and Propagation*, AP-48, No. 9, 2000, pp.1326–1339.

[35] Chew, W.C., *Waves and Fields in Inhomogeneous Media*, Piscataway, NJ, IEEE Press, 1995.

[36] Stratton, J.A., *Electromagnetic Theory*, New York, McGraw-Hill, 1941.

[37] Marcatili, E.A.J. and Schmeltzer, R.A., 'Hollow Metallic Dielectric Waveguides for Long Distance Optical Transmission and Lasers', *Bell System Technical Journal*, 43, 1964, pp.1783–1809.

[38] Wait, J.R., 'A Fundamental Difficulty in the Analysis of Cylindrical Waveguides with Impedances Walls', *Electronics Letters*, No. 3, 1967, pp.87–88.

[39] Emslie, A.G., Lagace, R.L., and Strong, P.F., 'Theory of Propagation of UHF Radio Waves in Coal Mine Tunnels', *IEEE Transactions on Antennas and Propagation*, AP-23, No. 2, 1975, pp.192–205.

[40] Mahmoud, S.F., 'Modal Propagation of High Frequency Electromagnetic Waves in Straight and Curved Tunnels within the Earth', *Journal of Electromagnetic Waves and Applications*, No. 19, 2005, pp.1611–1627.

[41] Lienard, M., Degauque, P., and Laly, P., 'Long Range Radar Sensor for Application in Railway Tunnels', *IEEE Transactions on Vehicular Technology*, AP-53, No. 3, 2004, pp.705–715.

[42] Loyka, S., 'Multichannel Capacities of Waveguide and Cavity Channels', *IEEE Transactions on Vehicular Technology*, AP-54, No. 3, 2005, pp.863–872.

[43] Lewin, L., Chang, D.C, and Kuester, E.F., *Electromagnetic Waves and Curved Structures*, Stevenage, England, Peter Pregrinus, 1977.

[44] Abramowitz, M., and Stegun, I.A., *Handbook of Mathematical Functions*, New York, Dover, 1970.

[45] Lienard, M., Degauque, P., Baudet, J., and Degardin, D., 'Investigation on MIMO Channels in Subway Tunnels', *IEEE J. on Selected Areas in Communications*, 21, No. 3, 2003, pp.332–339.

[46] Hartmann, C.S., "A global SAW ID tag with large data capacity", Ultrasonics Symposium, Vol 1, pp 65-69, 2002.

[47] Julian W. Gardner, Vijay K. Varadan and Osama O. Awadelkarim, Microsensors, MEMS and Smart Devices, John Wiley & Sons, LTD, ISBN 0-471-86109-X, 2002.

[48] Dunn, S.; Whatmore, R.W. "Transformation dependence of lead zirconate titanate (PZT) as shown by PiezoAFM surface mapping of sol-gel produced PZT on various substrates", Integrated Ferroelectrics, vol.38, no.1-4, pp. 39-47, 2001.

[49] Reindle, L.; Scholl, G.; Ostertag, T.; Ruppel, C.C.W.; Bulst, W.-E.; Seifert, F., "SAW Devices as Wireless Passive Sensors", Ultrasonics Symposium, Vol 1, no.1-4, pp. 363-367, 1996.

[50] Ostermayer, G.; Pohl, A.; Hausleitner, C.; Reindl, L.; Seifert, F., "CDMA for Wireless SAW Sensor Applications", Proc. IEEE Symp. on Spread Spectrum Techniques & Applications, pp. 795-799, 1996.

[51] Schmidt, F.; Sczesny, O.; Reindl, L.; Magori, V., "Remote sensing of physical parameters by means of passive surface acoustic wave devices ("ID-TAG")", Proc. IEEE Ultrasonics Symp., pp. 589-592, 1994.

[52] Bulusu, N.; Heidemann, J.; Estrin, D., "GPS-less low-cost outdoor localization for very small devices", Personal Communications, Vol 7, Issue 5, pp. 28-34, 2000.

[53] R. Bridgelall, "Characterization of Protocol-Compatible Bluetooth/802.11 RFID Tags," *RFDesign*, pp. 34-46, July 2002.

BIOGRAPHICAL INFORMATION

Darmindra D. Arumugam is a Researcher with the Texas Radio Frequency Innovation and Technology Center at the University of Texas at Arlington. He is a Graduate Research Assistant and a Graduate Student in the Department of Electrical Engineering at UTA. He received a BSc in Electrical Engineering and is currently pursuing an MSc at the UTA. His current research is in the area of Radio Frequency Identification (RFID) system design, applications of RFID, RFID antennae design, system-level modeling of RFID systems, energy harvesting, wireless sensor networks and intelligent objects. Mr. Arumugam's vision is to create a world pervaded with ambient intelligence that would radically rethink the interaction between humans and objects or machines. His near term vision is to help foster a more immersive relationship between intelligent objects and humans and help both entities expand their minds and thought processes.